

# The Epidermal Microbiome Within An Aggregation of Leopard Sharks (*Triakis semifasciata*) Has Taxonomic Flexibility With Gene Functional Stability Across Three Time-Points

Michael Doane (✉ [michael.doane@flinders.edu.au](mailto:michael.doane@flinders.edu.au))

Flinders University <https://orcid.org/0000-0001-9820-2193>

Colton Johnson

San Diego State University

Shaili Johri

Stanford University

Emma N. Kerr

Flinders University

Megan M. Morris

Laurence Livermore National Labs

Ric Desantiago

San Diego State University

Abigail C. Turnlund

University of Queensland

Asha Goodman

San Diego State University

Maria Mora

San Diego State University

Laís Farias Oliveira Lima

San Diego State University

Andrew P. Nosal

University of San Diego

Elizabeth A. Dinsdale

San Diego State University

---

## Research

**Keywords:** Microbiome, leopard shark, *Triakis semifasciata*, shark skin, next-generation sequencing

**Posted Date:** November 2nd, 2021

**DOI:** <https://doi.org/10.21203/rs.3.rs-850465/v2>

**License:**  This work is licensed under a Creative Commons Attribution 4.0 International License.

[Read Full License](#)

---

**Version of Record:** A version of this preprint was published at Microbial Ecology on February 7th, 2022.

See the published version at <https://doi.org/10.1007/s00248-022-01969-y>.

1 **The epidermal microbiome within an aggregation of leopard sharks (*Triakis semifasciata*)**  
2 **has taxonomic flexibility with gene functional stability across three time-points**

3 Michael P. Doane<sup>1#</sup>, Colton Johnson<sup>2#</sup>, Shaili Johri<sup>3</sup>, Emma N. Kerr<sup>1</sup>, Megan M. Morris<sup>4</sup>, Ric  
4 Desantiago<sup>2</sup>, Abigail C. Turnlund<sup>5</sup>, Asha Goodman<sup>2</sup>, Maria Mora<sup>2</sup>, Laís Farias Oliveira Lima<sup>2</sup>,  
5 Andrew P. Nosal<sup>6,7</sup>, Elizabeth A. Dinsdale<sup>2</sup>

6  
7 <sup>1</sup>College of Science and Engineering, Flinders University, Bedford Park, South Australia,  
8 Australia

9 <sup>2</sup>Department of Biology, San Diego State University, San Diego, California, USA

10 <sup>3</sup>Hopkins Marine Station, Stanford University, Pacific Grove, California, USA

11 <sup>4</sup>Laurence Livermore National Labs, Livermore, California, USA

12 <sup>5</sup>Australian Centre for Ecogenomics, University of Queensland, St Lucia, Queensland, Australia

13 <sup>6</sup>Department of Environmental and Ocean Sciences, University of San Diego, San Diego,  
14 California, USA

15 <sup>7</sup>Scripps Institution of Oceanography, University of California – San Diego, La Jolla, California,  
16 USA

17 #co-first authors

18

19 Michael P. Doane: 0000-0001-9820-2193

20 **michael.doane@flinders.edu.au**

21 Colton Johnson: 0000-0001-8895-6813

22 **cjohnson1412@sdsu.edu**

23 Shaili Johri: 0000-0001-7481-7548

24 **shailij@stanford.edu**

25 Emma N. Kerr

26 **Emma.n.kerr@gmail.com**

27 Megan M. Morris: 0000-0002-7024-8234

28 **morris81@llnl.gov**

29 Ricardo Desantiago

30 **rdesantiago@sdsu.edu**

31 Abigail C. Turnlund  
32 **acturnlund@gmail.com**  
33 Asha Z. Goodman  
34 **azgoodman@sdsu.edu**  
35 Maria F. Mora  
36 **moramariaf21@gmail.com**  
37 Laís Farias Oliveira Lima: 0000-0002-7616-3637  
38 **laisfolima@gmail.com**  
39 Andrew P. Nosal: 0000-0002-1815-9269  
40 **anosal@ucsd.edu**  
41 Elizabeth A. Dinsdale: 0000-0002-2177-203X  
42 **elizabeth.dinsdale@flinders.edu.au**  
43  
44  
45  
46  
47  
48  
49  
50  
51  
52  
53  
54  
55  
56  
57  
58

59 **The epidermal microbiome within an aggregation of *Triakis semifasciata* (leopard shark)**  
60 **has taxonomic flexibility with gene functional stability across three time-points**

61 Michael P. Doane<sup>1#</sup>, Colton Johnson<sup>2#</sup>, Shaili Johri<sup>3</sup>, Emma N. Kerr<sup>1</sup>, Megan M. Morris<sup>4</sup>, Ric  
62 Desantiago<sup>2</sup>, Abigail C. Turnlund<sup>5</sup>, Asha Goodman<sup>2</sup>, Maria Mora<sup>2</sup>, Laís Farias Oliveira Lima<sup>2</sup>,  
63 Andrew P. Nosal<sup>6,7</sup>, Elizabeth A. Dinsdale<sup>2</sup>

64

65 <sup>1</sup>College of Science and Engineering, Flinders University, Bedford Park, South Australia,  
66 Australia

67 <sup>2</sup>Department of Biology, San Diego State University, San Diego, California, USA

68 <sup>3</sup>Hopkins Marine Station, Stanford University, Pacific Grove, California, USA

69 <sup>4</sup>Laurence Livermore National Labs, Livermore, California, USA

70 <sup>5</sup>Australian Centre for Ecogenomics, University of Queensland, St Lucia, Queensland, Australia

71 <sup>6</sup>Department of Environmental and Ocean Sciences, University of San Diego, San Diego,  
72 California, USA

73 <sup>7</sup>Scripps Institution of Oceanography, University of California – San Diego, La Jolla, California,  
74 USA

75

76 **Abstract**

77 *Background:* The epidermis of Chondrichthyan fishes consists of dermal denticles with  
78 production of minimal but protein rich mucus that influence the attachment and biofilm  
79 development of microbes, facilitating a unique epidermal microbiome. Here, we use  
80 metagenomics to provide the taxonomic and functional characterization of the epidermal  
81 microbiome of the *Triakis semifasciata* (leopard shark) across three time-points to identify links  
82 between microbial groups and host metabolism. Our aims include 1) describing the variation of  
83 microbiome taxa over time and identify those members which are recurrent (present across all  
84 time-points, 2) investigating the relationship between the recurrent and flexible taxa (those which  
85 are not found consistently across time-points, 3) describing the functional compositions of the  
86 microbiome which may suggest links with the host metabolism; and 4) identifying whether the  
87 metabolisms are share across microbial genera or found in specific taxa.

88

89 *Results:* Microbial members of the microbiome showed high similarity between all individuals  
90 (average similarity: 82.74) with relative abundance of those members varying across years,

91 suggesting flexibility of taxa in the microbiome. One hundred and eighty-eight genera were  
92 identified as recurrent, including *Pseudomonas*, *Erythrobacter*, *Alcanivorax*, *Marinobacter* and  
93 *Sphingopxis* being consistently abundance across time-points, while *Limnobacter* and *Xyella*  
94 exhibited switching patterns with high relative abundance in 2013, *Sphingobium* and  
95 *Sphingomona* in 2015, and *Altermonas*, *Leeuwenhoekiella*, *Gramella* and *Maribacter* in 2017. Of  
96 the 188 genera identified as recurrent, the top 19 relative abundant genera forming three  
97 recurrent groups. The microbiome also displayed high functional similarity between individuals  
98 (average similarity: 97.65) with gene function composition being consistent across time-points.  
99

100 *Conclusion:* These results show that while presence of microbial genera exhibit consistency  
101 across time-points, their abundances do fluctuate. Functions however remain stable across time  
102 points; thus, we suggest the leopard shark microbiomes exhibit functional redundancy. We  
103 hypothesize this may be the result of the host's epidermal attributes structuring the microbiome.  
104 In addition, we show the co-existence of many microbial genera that carry genes which may  
105 enable the microbes to use the nutrients provided by the elasmobranch's metabolism.  
106

107 **Keywords:** Microbiome, leopard shark, *Triakis semifasciata*, shark skin, next-generation  
108 sequencing

## 109 **Introduction**

110 The epidermis of marine organisms is biologically active (i.e. not keratinised like most terrestrial  
111 organisms)(Meyer and Seegers 2012), serving as the first line of defence against environmental  
112 influences. Along with providing broad protections, the skin of elasmobranchs interacts with the  
113 microbes from the surrounding environment, forming a specific microbiome (Doane et al.,  
114 2017). The epidermal microbiome of five elasmobranchs, including thresher sharks (*Alopias*  
115 *vulpinus*), whale sharks (*Rhincodon typus*), leopard sharks (*Triakis semifasciata*), blacktip reef  
116 sharks (*Carcharhinus melanopterus*), and round rays (*Urobatis helleri*) confirmed that the  
117 elasmobranch epidermal microbiomes are species-specific (Doane et al. 2017; Doane et al. 2020;  
118 Pogoreutz et al. 2019). However, the selection and maintenance of the microbiome on sharks  
119 remains an outstanding question, and may be the result of several processes, including 1)

120 biophysical properties of the epidermis, 2) epidermal secretions of the shark, and 3) interspecific  
121 interactions between the microbes.

122

123 The biophysical properties of the chondrichthyan fish epidermis are uniquely covered with  
124 dermal denticles that improve hydro-dynamism (Lang 2020). Dermal denticles have ridges and  
125 troughs arranged in overlapping patterns that alter the hydrodynamic properties of water close to  
126 the epidermis (Sullivan and Regan 2011b; Zhang et al. 2011; Wen et al. 2015) and this  
127 biophysical property potentially affects microbial growth. In synthetic models mimicking shark  
128 skin, two bacteria, *Escherichia coli* and *Staphylococcus aureus*, showed differential growth  
129 patterns compared to a smooth surface. *E. coli* had high attachment rates to the structure surface,  
130 whereas *S. aureus* was not able to attach (Chien et al. 2020), therefore, suggesting that only  
131 specific types of microbes are able to attach to the shark skin. Further, modeling of microbial  
132 community dynamics shows that high surface structural complexity can reduce competition  
133 between microbes that result in chaotic spatial species distribution pattern on the surface  
134 (Lowery and Ursell 2019). Therefore, the high micro-structured nature of the shark skin surface,  
135 may produce similar dynamics in the microbiome. Further, the epidermis of Chondrichthyan fish  
136 is characterized by a lower level of secretory cells compared with Actinopterygian fishes (Meyer  
137 and Seeger 2012) and the product is a thin heterogeneous outer mucous layer (5–8  $\mu\text{m}$  thickness;  
138 pH between 6 and 7). The mucus contains high levels of proteins, with only one protein being  
139 identified, which is lectin pentraxin (Tsutsui et al. 2014) and has moderate to high disulphide  
140 concentrations that is suspected to provide mechanical stabilization of the mucus coating (Meyer,  
141 Seegers, and Stelzer 2007).

142

143 The metabolism of Elasmobranchs may also affect the functions of the microbiomes in the form  
144 of secretions being transported by the skin mucus. Elasmobranchs rely on ketone bodies, fatty  
145 acids, carbohydrates, and amino acids for energy production (Speers-Roesch and Treberg 2010).  
146 Amino acids are ketogenic precursors, oxidative fuel, and nitrogen suppliers (Speers-Roesch and  
147 Treberg 2010). Nitrogen metabolism is also important due to the high amount of urea  
148 synthesised for osmoregulation, along with trimethylamine N-oxide (TMAO), which could also  
149 be transported to the skin surface via mucus production (Ballantyne 1997; Speers-Roesch and  
150 Treberg 2010). Sharks bioaccumulate toxins and heavy metals from lower trophic levels

151 (Escobar-Sanchez, Galvan-Magana, and Rosiles-Martinez 2010; Maz-Courrau et al. 2012) and  
152 have been shown to exhibit maternal off-loading to their offspring in mucus surrounding  
153 developing embryo (Lyons and Lowe, 2013). Therefore, metabolically derived compounds and  
154 harmful contaminants are being leached from elasmobranchs in their mucus and if this occurs at  
155 the skin surface may structure the skin microbiome. For instance, the microbiome signature from  
156 thresher sharks (*Alopias vulpinus*) suggests potential heavy metal concentration at the skin  
157 interface signified by high abundance of heavy metal resistance genes (Doane et al., 2017).

158  
159 Interactions between the microbes on the surface and those from the surrounding water are also  
160 expected to affect the characteristics of the microbiome. The low levels of mucus secreted by the  
161 sharks and minimal biofilm development that occurred on the synthetic models of the shark skin,  
162 compared with the pronounced biofilm development on the smooth surface (Chien et al. 2020),  
163 suggests that microbial growth on the epidermis is suppressed, and the turnover of microbial  
164 communities may be high. Conversely, stability of a microbiome is important for the host's  
165 health and functioning, and rapid or unexpected variations in microbiome taxonomy leads to a  
166 state of dysbiosis, which can result in a decline in organismal health (Costello et al. 2012; Egan  
167 and Gardiner 2016). Therefore, an understanding of how the microbiome varies through time is  
168 important, but there are limited investigations of microbiome stability over time in the marine  
169 environment. A few examples include the epidermis microbiome of humpback whales  
170 (*Megaptera novaeangliae*) and Atlantic cod (*Gadus morhua*) which varied seasonally (Bierlich  
171 et al. 2018; Wilson, Danilowicz, and Meijer 2008), and similar seasonal changes occurred in the  
172 microbiome of the stony coral, *Montastrea faveolata* (Kimes et al. 2013). While the respiratory  
173 microbiome of bottlenose dolphin species (*Tursiops truncatus* and *Tursiops aduncus*) maintained  
174 taxonomic stability over two months, but individual dolphins had significantly different  
175 microbiome taxonomic structures (Lima et al. 2012). In an analysis of 8 months, captive  
176 dolphins had an individual signature of their lung microbiome and shared between 17 – 41 % of  
177 the microbiome with other individuals (Vendl et al. 2021). In contrast, 77.6 % of the microbes in  
178 the epidermal microbiome of thresher sharks (*A. vulpinus*) were shared across individual sharks  
179 (Doane et al. 2017), however, this study was only conducted at one timepoint. Therefore,  
180 whether the epidermal microbiomes of marine vertebrate hosts are temporal stable or flexible  
181 remains an outstanding question in science.

182

183 Here we analyse both the taxonomic make-up and functional capabilities of the leopard shark  
184 (*Triakis semifasciata*) epidermal microbiome over five years (three sampling time-points) using  
185 the following objectives: 1) to describe the variation of microbiome taxa over time and identify  
186 those members which are recurrent (present across time-points, 2) to investigate the relationship  
187 between the recurrent and flexible taxa (those which are not found consistently across time-  
188 points, 3) to describe the functional compositions of the microbiome which may suggest links  
189 with the host metabolism; and 4) to identify whether the metabolisms are share across microbial  
190 genera or found in specific taxa.

191

## 192 **Materials and Methods**

### 193 *Epidermal Microbiome Sampling*

194 Leopard sharks (*Triakis Semifasciata*) sharks form consistent aggregations in late summer, early  
195 fall at near-shore locations (Nosal et al. 2014; Nosal et al. 2013) along the coast of California  
196 making this species a good candidate to investigate temporal microbiome dynamics of a wild  
197 animal. Sharks in this study were sampled from La Jolla Cove, California, USA (32°51'12" N,  
198 117°15'48" W). We targeted at least three sharks per year, and captured eight sharks in 2013,  
199 three in 2015, and seven in 2017, thus the study was conducted over a five-year period. The  
200 sharks were caught with a handline on baited barbless circle hooks and brought onboard a small  
201 skiff for processing using a scoop net; all sharks were released after processing. Microbiome  
202 samples from the sharks were collected using a microbial collection tool, which flushes the  
203 epidermis with ~250 ml of sterile seawater and dislodges the microbes. The microbial slurry is  
204 collected into the back end of the microbial tool, as we have conducted previously (Doane et al.  
205 2017; Doane et al. 2018; Doane et al. 2020; Johri et al. 2019; Lima et al. 2020). Each epidermal  
206 microbiome sample was taken from the flank region below the dorsal fin and above the lateral  
207 line. The collected microbiome samples were filtered through a 0.22 µm Sterivex filter  
208 (Millipore, Inc.) and stored in a -20 °C freezer until processing.

209

### 210 *DNA Extraction and Sequencing*

211 Microbiome DNA was extracted using a cell lysis and spin-column filtration method by  
212 Macherey Nagel Tissue Kit. The purified DNA was prepared for random shot-gun sequencing

213 using the standard protocol from Swift 2S Plus Kit (Swift Biosciences). The DNA library was  
214 sequenced using a Mi-Seq Illumina sequencer with Mi-Seq v3 Reagent Kit. Samples were bar-  
215 coded and the *T. semifasciata* microbiomes were mixed in with a range of microbiome samples  
216 and run on several sequencing runs.

217

### 218 *Metagenome Annotation*

219 The sequenced metagenomes were processed through PRINSEQ $\pm\pm$  software for quality control,  
220 removing sequences less than 70 bp, those that had a single N, or a quality score below 25. MID  
221 tags were also removed with PRINSEQ $\pm\pm$  (Cantu, Sadural, and Edwards 2019; Schmieder and  
222 Edwards 2011). The two fasta files were paired using FLASH software (Magoc and Salzberg  
223 2011). After pairing, metagenomes were uploaded into MG-RAST Version 4.0.3, which was  
224 used to provide taxonomic and functional gene annotations of the metagenomes using standard  
225 cut-offs (Aziz et al. 2008; Meyer et al. 2008). The sequences with the highest bit score were  
226 reported. The taxonomic annotation outputs were filtered in MG-RAST to only include those  
227 from Bacteria and Archaea domains. Viruses and Eukaryotes were not used in the analysis  
228 because they were underrepresented in the metagenome. The functional gene characterization  
229 was obtained from the SEED platform (Overbeek et al. 2005), similar to previous analysis  
230 (Dinsdale, Edwards, et al. 2008; Dinsdale, Pantos, et al. 2008).

231

### 232 *Quantitative evaluation of leopard shark microbiomes*

233 To identify whether the taxonomy of the microbiome remained consistent or varied over time, a  
234 Permanova on the relative abundance of each taxon level was conducted across years (Anderson  
235 2017). All data was fourth root transformed to reduce abundance variation among samples. A  
236 simpler analysis was used to identify the taxa contributing to the dissimilarity between years  
237 (Clarke, Somerfield, and Gorley 2008). A principal coordinate analysis was performed on the  
238 taxonomic data to visualize the variation in the structure of the microbiomes over the years.  $\beta$ -  
239 diversity was identified using a Bray-Curtis analysis with 100 - similarity index, where 0 = high  
240 overlap, 100 = no overlap. Last, a PERMDISP analysis compared the distribution of microbial  
241 taxa across each year around the year's group centroid (Clarke, Somerfield, and Gorley 2016;  
242 Anderson 2006).

243  
244 We identified a recurrent group of microbes (or core) as those genera that were present on every  
245 individual shark, on a presence/absence basis and non-recurrent microbes, as all other genera that  
246 were an occasional member of the microbiome. The 19 most abundant recurrent and non-  
247 recurrent microbial taxa (abundances calculated within the recurrent/non-recurrent datasets,  
248 separately) were compared with a Bray-Curtis similarity analysis to identified groups of genera  
249 that had a similar proportional abundance across years. A Pearson correlation was conducted to  
250 identify positive or negative correlations between these taxonomic groupings. The output of the  
251 Pearson correlation was organized into a heatmap and combined with the Bray-Curtis  
252 dendrogram. The analysis identified negative and positive correlations between the microbial  
253 groups that live on the shark epidermis.

254  
255 To identify whether the functional potential of the shark epidermis microbiome remains stable or  
256 varies temporally, a PERMANOVA was conducted to compare variation in functional  
257 components across years. The SEED provides a hierarchal description including major  
258 metabolisms, metabolic pathways, gene clusters and gene functions (Overbeek et al. 2005). The  
259 SIMPER analysis identified potential functions that contributed to the dissimilarity between  
260 years. A principal coordinate analysis was performed to visualize the variation in the functional  
261 potential of the microbiomes over the years and a PERMDISP analysis compared the distribution  
262 of functional potential of *T. semifasciata* epidermal microbiome across years. All analyses were  
263 performed in PRIMER Version 6.1.15 & PERMANOVA± Version 1.0.5 from PRIMER-E  
264 (2012). GraphPad Prism Version 8.3.1 was used to visualize the data.

265  
266 We identified the functional potential of the 17 most proportionally abundant genera using the  
267 Krona plug-in (Ondov, Bergman, and Phillippy 2011) in MG-RAST (Aziz et al. 2008; Meyer et  
268 al. 2008). Only 17 genera were use because they occurred in sufficient abundance to explore the  
269 functions of the genera. The sequences were further investigated using Kyoto Encyclopedia of  
270 Genes and Genomes (KEGG) Orthology (KO) database's KEGG mapper plug-in on MG-RAST  
271 (Kanehisa et al. 2012; Kanehisa et al. 2016), which provided identification of metabolic and  
272 biochemical pathways. The proportion of sequences within each genus for each functional group  
273 was calculated as the number of sequences within a genus divided by the total number of

274 sequences within the function across the 17 genera. The proportion of sequences associated with  
275 each function in each genus was categorized into one of four quartiles: < 75 %, 50 – 75 %, 25 –  
276 50 %, 1 – 25 %, and 0 % and visualized using a heatmap. The heatmap was used to visualize the  
277 connection between the microbes and the sharks over time and identified whether there was  
278 switching of specific functional roles between genera in the microbiome.

279

## 280 **Results**

### 281 *Temporal Taxonomy of the Epidermal Microbiome*

282 The epidermal microbiomes were constructed from 18 *T. semifasciata*, including seven  
283 individuals in 2013, three in 2015 and eight in 2017 caught in La Jolla, California. Metagenomes  
284 ranged from 312,135 – 2,347,886 sequences that had 89,080,935 – 605,042,370 base pairs (Table  
285 1). Of those sequences identified as protein coding, 24.01 – 83.74 % were classified as unknown  
286 sequences, which could not be matched to database (Table 1). The abundant phyla represented in  
287 the *T. semifasciata* epidermal microbiome were Proteobacteria ( $78.50 \pm 2.02$  S.E. %),  
288 Bacteroidetes ( $15.83 \pm 2.34$  %), and Actinobacteria ( $2.09 \pm 0.30$  %). Within the Proteobacteria  
289 the classes Gammaproteobacteria ( $38.99 \pm 2.28$  %) and Alphaproteobacteria ( $31.32 \pm 2.20$  %)  
290 were evenly represented, with Betaproteobacteria ( $7.25 \pm 0.81$  %) and Deltaproteobacteria ( $0.81$   
291  $\pm 0.05$  %) in lower relative abundance (SI Figure 1). Within the Bacteroidetes, the Flavobacteria  
292 class made up 12.08 % ( $\pm 2.15$ ) of the metagenome and Actinobacteria class accounted for 2.40  
293 % ( $\pm 0.30$ ) (SI Figure 2).

294 Across the 18 leopard sharks, 597 genera made up the epidermal microbiome. Highly  
295 represented genera present within the microbiomes included *Pseudomonas* ( $9.85 \pm 1.81$  %),  
296 *Erythrobacter* ( $5.88 \pm 0.69$  %), *Leeuwenhoekiella* ( $2.52 \pm 0.72$  %), and *Limnobacter* ( $1.51 \pm 0.42$   
297 %) (Figure 1). The *T. semifasciata* microbiomes collected across the three time-points showed  
298 high taxonomic similarity between all individuals, with average Bray-Curtis similarity of 82.74  
299 (0 = no overlap, 100 = total overlap) among all pairs of samples. The similarity of the genera on  
300 the sharks across time-points suggests a selective process is occurring and that the shark  
301 epidermis has a specialized microbiome (Figure 1). The 19 most relative abundant genera  
302 (except for *Providencia*  $2.29 \pm 0.94$  %) were recurrent over sampling periods, but the  
303 proportional abundance varied throughout the years (Figure 3). The PERMANOVA analysis  
304 identified significant differences in the proportional abundances of all taxonomic levels between

305 years (PERMANOVA: Phylum, Pseudo-F<sub>df=2</sub> = 3.696, P(perm) = 0.001; Class, Pseudo-F<sub>df=2</sub> =  
306 3.628, P(perm) = 0.001; Order, Pseudo-F<sub>df=2</sub> = 3.222, P(perm) < 0.01; Family, Pseudo-F<sub>df=2</sub> =  
307 2.762, P(perm) < 0.01; Genus, Pseudo-F<sub>df=2</sub> = 2.967, P(perm) = 0.049). The microbial genera of  
308 the *T. semifasciata* epidermal microbiomes formed distinct clusters for each year in the principal  
309 coordinate analysis, which explained 64.7 % of the variation in the first two axes (Figure 2). A  
310 few outliers identified in 2013 and 2017 may be associated with variation in an individual  
311 shark's physiology, i.e., such as pregnancy.

312 The SIMPER analysis identified a similarity coefficient of 83.05 between 2013 & 2015; 80.29  
313 for 2013 & 2017; and 84.64 for 2015 & 2017 (Bray-Curtis similarity index, 100 = similar, 0 = no  
314 overlap). Genera of the Gammaproteobacteria class contributed the most to the dissimilarity  
315 between the years, followed by genera in the Alphaproteobacteria and Betaproteobacteria, and  
316 the Flavobacteria class from the Bacteroidetes phylum (Table 2). The variation in the relative  
317 abundance of *Alcanivorax* and *Alteromonas* contributed the most to the dissimilarity across  
318 years.

319 Last, we explored the variance within years of microbial taxonomy with PERMDISP analysis.  
320 Each year the microbiome showed a similar amount of variation within the microbiomes at each  
321 taxonomic level (PERMDISP: Phylum, F<sub>df=2, 15</sub> = 2.120, P(perm) > 0.1; Class, F<sub>df=2, 15</sub> =  
322 2.439, P(perm) > 0.1; Order, F<sub>df=2, 15</sub> = 1.513, P(perm) > 0.5; Family, F<sub>df=2, 15</sub> = 2.019, P(perm)  
323 > 0.1; Genus, F<sub>df=2, 15</sub> = 2.142, P(perm) > 0.05). The microbiomes from 2013, 2015, and 2017  
324 showed a dispersion of 11.7 (± 1.8), 6.0 (± 0.8), and 10.1 (± 1.3) respectively. In summary, the  
325 individual sharks shared many microbial genera suggesting a consistent taxon across the years,  
326 with flexibility in the proportional abundance.

### 327 *Temporally Recurrent Microbes*

328 Microbial genera present in all 18 metagenomes, were categorized as 'recurrent' which included  
329 188 of 597 genera. The stability was considered further by comparing the proportional  
330 abundance of sequences within the 188 genera across sampling periods and identified a  
331 significant difference (PERMANOVA: Pseudo-F<sub>df=2, 15</sub> = 10.462, P(perm) = 0.001). The  
332 variability in the recurrent microbial genera, measured by PERMDISP (PERMDISP: F<sub>df=2, 15</sub> =  
333 0.029, P(perm) = 0.983) indicated no difference across years with 2013, 2015, and 2017 showing  
334 a dispersion of 4.09 (± 0.47), 4.07 (± 0.57), 3.974 (± 0.22), respectively. Collectively the

335 fluctuations in the dominate genera along with similar variability across time suggest a flexible  
336 but regulated recurrent groups of microbes in the *T. semifasciata* microbiome.

337

### 338 *Relationship between recurrent and non-recurrent genera*

339 In the clustering analysis, the 19 dominant recurrent microbes formed three groups and the 19  
340 non-recurrent microbes formed five separate groups (Figure 4). The recurrent group A consisted  
341 of *Pseudomonas*, *Erythrobacter*, *Alcanivorax*, and *Marinobacter*, which showed an even  
342 proportional abundance across the five years and with *Erythrobacter* and *Marinobacter* having  
343 higher proportional abundance in 2013. The recurrent group B consisted of seven genera which  
344 showed higher proportional abundance in 2017 and included *Leeuwenhoekiella*, *Altermonas*,  
345 *Gramella*, *Zunongwangia*, *Pseudoaltermonas*, *Flabacterium*, and *Maribacter*. The recurrent  
346 group C consisted of six genera with lower proportional abundance, including *Burkholderia*,  
347 *Novoshingobium* and *Sphingopyxis*, which showed even distribution across the years, *Rugeria*,  
348 which showed proportional higher abundance in 2013 and 2017 and *Sphingobium* and  
349 *Sphingomonas*, which showed higher proportional abundance in 2015. The non-recurrent (top 19  
350 most relative abundant genera not occurring across all sampling points) microbial group A  
351 consisted of three genera with lower proportional abundance in 2017, including  
352 *Propionibacterium*, *Pirellula*, and *Plesiocystis*. The non-recurrent microbial group B consisted of  
353 two genera that showed low but even proportional abundance across all years and included  
354 *Aromatoleum* and *Chromobacterium*. The non-recurrent microbial group C only consisted of  
355 *Dokdonia*, which displayed higher proportional abundance in 2017. The non-recurrent group D  
356 included *Acidiphillium*, *Azorhizobium*, *Gluconobacter*, and *Sphingobacterium* and the first two  
357 genera displayed low even proportional abundances throughout all years *Gluconobacter* and  
358 *Sphingobium* showed higher proportional abundance in 2017. The non-recurrent microbial group  
359 E, including *Leadbetterella*, *Klebsiella*, *Neisseria*, *Oligotropha*, *Thauara*, and *Frankia*.  
360 *Leadbetterella* displayed its highest proportional abundance in 2015. *Klebsiella*, *Neisseria*, and  
361 *Thauara* showed even proportional abundance across all years. *Oligotropha* and *Frankia*  
362 displayed lower proportional abundances at all years (Figure 4). There also occurred a clustering  
363 group termed ‘mixed’ because genera included those which were classified as both recurrent and  
364 non-recurrent including *Endoritia*, *Limnobacter*, *Xylella*, and *Providencia* genera.

365 We then investigated the correlative relationship of recurrent and non-recurrent groups (Figure  
366 4). The heatmap showed that *Erythrobacter* and *Marinobacter* (recurrent group A) were  
367 negatively correlated with all microbes in recurrent group B. Whereas *Pseudomonas* and  
368 *Alcanivorax* (recurrent group A) showed positive correlations with recurrent group B. Recurrent  
369 group A, however, was positively correlated with non-recurrent group A and B. In contrast,  
370 recurrent group B was negatively correlated with non-recurrent group A and B but strongly  
371 associated with non-recurrent group C, *Dokdonia*. Recurrent group C was positively correlated  
372 with non-recurrent groups A, B, D, E, and the mixed group (Figure 4). These associations  
373 between taxa will be investigated further in the functional analysis to identify metabolisms that  
374 may drive the microbiome composition.

#### 375 *Functional potential of the shark epidermis microbiome*

376 Annotated microbial sequences were categorized into 26 major metabolic groups, 153 metabolic  
377 pathways, 949 functional gene clusters, and 5,358 functional genes. The gene function profiles  
378 were highly stable across the three time-points as evidenced by the high functional similarity  
379 between individual sharks (mean 97.65, Bray-Curtis similarity index). There was not a  
380 significant difference between time-points in the functional potential of the microbiome  
381 (PERMANOVA: major metabolic groups, Pseudo-F<sub>df=2, 15</sub> = 1.8, P(permutation) > 0.05; metabolic  
382 pathways, Pseudo-F<sub>df=2, 15</sub> = 0.525, P(permutation) > 0.5; functional gene clusters, Pseudo-F<sub>df=2, 15</sub> =  
383 1.182, P(permutation) > 0.1). The similarity of the functional potential was shown by the single cluster  
384 on the principal coordinate analysis that explained 64.4 % of the variation in the first two axes  
385 (Figure 5).

386 The major metabolic groups included carbohydrates (mean  $10.96 \pm 0.32$  %); amino acids &  
387 derivatives ( $9.17 \pm 0.19$  %); protein metabolism ( $7.88 \pm 0.11$  %); and fatty acids, lipids, &  
388 isoprenoids ( $2.61 \pm 0.04$  %) (SI Figure 3). In nitrogen metabolism ( $1.23 \pm 0.11$  %), there were 11  
389 functional gene clusters in the microbiome including ammonia assimilation ( $0.51 \pm 0.01$  %),  
390 nitrate and nitrite ammonification ( $0.38 \pm 0.001$  %), and denitrification ( $0.10 \pm 0.02$  %), but few  
391 sequences were associated with nitrogen fixing genes ( $0.02 \pm 0.007$  %) suggesting high levels of  
392 organic nitrogen that are present on the shark. Urea decomposition ( $0.27 \pm 0.02$  %) was present  
393 and there were a few sequences associated with trimethylamine N-oxide (TMAO) reductase  
394 ( $0.004 \pm 0.001$  %). The functional gene clusters that perform fatty acid biosynthesis and

395 metabolism are fatty acid biosynthesis FASII ( $0.72 \pm 0.02 \%$ ), fatty acid degradation regulons  
396 ( $0.22 \pm 0.02 \%$ ), and fatty acid metabolism ( $0.13 \pm 0.01 \%$ ). The functional gene clusters that  
397 complete protein biosynthesis and degradation are ATP dependent proteolysis in bacteria ( $0.37 \pm$   
398  $0.01 \%$ ), bacterial proteasome ( $0.30 \pm 0.02 \%$ ), protein degradation ( $0.20 \pm 0.01 \%$ ), nucleolar  
399 protein complex ( $1.01 \pm 0.05 \%$ ), aminopeptidase ( $0.18 \pm 0.01 \%$ ), metalloprotease ( $0.04 \pm 0.006 \%$ ),  
400 and bacterial ribosome LSU ( $0.38 \pm 0.02 \%$ ). A high proportional abundance  
401 of flagellar motility ( $1.27 \pm 0.06 \%$ ) and lower proportional abundance of bacterial chemotaxis  
402 ( $0.36 \pm 0.02 \%$ ) is consistent with low biofilm formation predicted on the shark epidermis. There  
403 was a high proportional abundance of functions associated with resistance to antibiotics and  
404 toxic compounds ( $5.08 \pm 0.13 \%$ ) and cobalt-zinc-cadmium resistance had a mean of  $1.58 \pm 0.12$   
405  $\%$ , multidrug resistance efflux pumps ( $0.85 \pm 0.05 \%$ ), copper homeostasis ( $0.69 \pm 0.05 \%$ ), and  
406 the production of exopolysaccharide biosynthesis (EPS) ( $0.058 \pm 0.008 \%$ ) and Rhamnolipids  
407 produced by *Pseudomonas* ( $0.005 \pm 0.002 \%$ ) that are used in heavy metal detoxification,  
408 consistent with bioaccumulation of heavy metals and toxins by the large-bodied sharks.

#### 409 *Microbial gene function across genera*

410 The 17 dominant recurrent genera were used to investigate whether functional genes were  
411 equally dispersed across the genera or confined to a small subset of microbes (Figure 6).  
412 *Pseudomonas*, had the highest proportion of sequences annotated to all metabolisms, including  
413 those involved in nitrate and nitrite ammonification and denitrification, and in association with  
414 *Alcanivorax*, also conducted ammonia assimilation. These two genera were positively correlated  
415 (Figure 6) with most other microbes, suggesting these were key functions in microbiome growth.  
416 In comparison, *Marinobacter* also specialized in these two functions plus urea decomposition  
417 and was negatively correlated *Pseudomonas* and *Alcanivorax*. *Ruegeria* and *Novosphingobium*  
418 were the only other genera that had a high proportion abundance of genes associated with urea  
419 decomposition, which may have caused the negatively correlated with recurrent group B. The  
420 genera within recurrent group B had a high proportion of genes associated with carbon  
421 metabolism, with *Gramella* having a high proportion of genes within TCA cycle, Glycolysis and  
422 Serine cycle. *Marinobacter* has a high proportion of genes in Glycolysis, Denitrification, and fatty  
423 acid biosynthesis. Many genera, including *Pseudomonas*, *Alcanivorax*, *Erythrobacter*,  
424 *Leeuwenhoekiella*, *Altermonas*, *Gramella* and *Flavobacterium*, had many sequences associated

425 with protein biosynthesis and degradation, and fatty acid biosynthesis, which are associated with  
426 the shark ketosis dominated metabolism. Genera within recurrent group C, including *Ruegeria*,  
427 *Sphingopyxis* and *Novosphingobium* had a high proportion of genes associated with  
428 Denitrification and fatty acid biosynthesis. All 17 genera, except 1, had sequences that matched  
429 the copper, cobalt and cambium resistance and copper homeostasis genes. The abundance of  
430 these functions across most genera in the metagenomes suggests the important heavy metal  
431 tolerance or manipulation for microbes living on the surface of sharks.

432

### 433 **Discussion**

434 The *T. semifasciata* epidermal microbiome was consistent between individual sharks with many  
435 genera shared across the three time-points spanning 5 years, one of the longest studies of marine  
436 vertebrate microbiomes to date. A recurrent set of 188 microbial genera were present on all  
437 individuals. However, there was flexibility in the proportional makeup of the microbiome across  
438 years, but the microbiome variability was consistent across years, suggesting similar ecological  
439 dynamics are occurring from year to year, despite some turnover in microbial genera. Regardless  
440 of the proportional abundance of each microbial genera, the functional potential was constant,  
441 suggesting that the epidermal microbes were responding to the unique environment of the *T.*  
442 *semifasciata* epidermis, including the dermal denticles that reduce biofilm build-up and  
443 potentially elements secreted via the minimal mucus associated with shark's metabolism.

444

#### 445 *Leopard shark microbiome exhibits specificity and flexibility*

446 The *T. semifasciata* epidermal microbiome has a high relative abundance of *Pseudomonas*,  
447 *Erythrobacter*, *Alcanivorax*, and *Marinobacter*; whereas the thresher shark (*Alopias vulpinus*)  
448 epidermal microbiome had a high relative abundance of *Pseudoalteromonas*, *Erythrobacter*,  
449 *Idiomarina*, and *Limnobacter* (Doane et al. 2017); and the *Carcharhinus*  
450 *melanopterus* epidermal microbiome a high relative abundance of *Psychrobacter*,  
451 *Pseudoalteromonas*, *Rhodobacter*, and *Alteromonas* (Pogoreutz et al. 2019). While some genera  
452 were shared across shark species, the proportional abundance differed, suggesting that each  
453 elasmobranch microbiome has distinct characteristics which select for differing microbiome  
454 members.

455  
456 The highly shared microbiome across individual sharks within a timepoint and flexible  
457 communities across timepoints coupled with evidence that species microbiomes are distinct may  
458 be caused by the dermal denticles (Chien et al. 2020; Dillon, Norris, and O'Dea 2017) and  
459 metabolites secreted in the skin mucus as a result of the sharks metabolism. Dermal denticles  
460 alter the hydrodynamic properties of water close to the epidermis, reducing drag on the shark  
461 (Sullivan and Regan 2011a) and micro-organism growth (Wen et al. 2015; Zhang et al. 2011). A  
462 study that tested the recruitment of two lab microbial species found that only one species was  
463 able to successfully recruit, and biofilms did not develop (Chien et al. 2020; Kim et al. 2012).  
464 Biofilm development is dependent on quorum sensing, which is interrupted on rough surfaces  
465 (Kim et al. 2012). We showed that specific microbial taxa recruit to the epidermis of *T.*  
466 *semifasciata* and the proportion of motility genes are relatively high compared to the chemotaxis  
467 genes which are proportionally low in abundance in the leopard shark microbiomes. These  
468 features are consistent across the microbiome of four shark species (Doane et al. 2017; Doane et  
469 al. 2020).

470  
471 Modelling of microbial community dynamics of surfaces with structural complexity, like the  
472 conditions on a sharkskin, potentially suggests there is lower interspecific competition, which  
473 results in a chaotic spatial distribution pattern of microbial species (Lowery and Ursell 2019).  
474 The *T. semifasciata* epidermal microbiome supports the modelling where 188 genera coexisted  
475 on all sharks across the three years, with flexibility in the relative abundance of those genera,  
476 suggesting that the epidermis may provide multiple niches for microbial taxa to survive. An  
477 emergent feature of the modelling is that competing genera do not go extinct (Lowery and Ursell  
478 2019), and we show that many microbial species co-occurred on the sharkskin across the three  
479 time-points. The co-occurrence or positive correlations within the microbiome suggest niche  
480 partitioning and sharing of resources with several genera exhibiting abundance relationships  
481 (Figure 4). For example, *Pseudomonas* and *Alcanivorax* showed positive correlations with  
482 recurrent group B members, including *Leeuwenhoekiella*, *Altermonas*, *Pseudoaltermonas*,  
483 *Flabacterium*, and *Maribacter*, suggesting that these two genera could share  
484 resources. *Erythrobacter* and *Marinobacter* were negatively correlated with all microbes in  
485 recurrent group B, suggesting strong competition; this group was however positively correlated

486 with non-recurrent group A and B, suggesting transient microbes add to the microbiome's growth  
487 at different years.

488

#### 489 *Microbiome functional groups*

490 We then investigated the gene functions present in the groups of microbial genera that may  
491 explain the positive or negative relationships between genera in Figure 4. In addition, because  
492 host metabolism and microbial functions are linked (Lynch and Hsiao 2019), we identified  
493 functional genes in each genus that may be linked to the host metabolism and classify three  
494 broad functional groups, generalists (recurrent group A), opportunists (recurrent group B) and  
495 specialists (recurrent group C) based on the presence of potential genes in these microbial  
496 genera. The group A recurrent microbes are typical marine species that have highly flexible  
497 genomes and growth strategies, including heterotrophic and photo-heterotrophic growth. These  
498 organisms can utilize many of the nutrients that may be present on the shark epidermis or  
499 excreted in the mucus, including proteins, fatty acids and disulphides (Meyer and Seegers 2012).  
500 *Pseudomonas*, for example, had the highest relative abundance and are capable of mixotrophy  
501 and simultaneous use of sulphur, nitrogen, and carbon from the surrounds (Guo, Chen, and Lee  
502 2019) and sequences similar to these genes were highly represented in the *Pseudomonas* in  
503 leopard shark microbiomes. *Pseudomonas* were positively correlation with many microbes  
504 (Figure 4), which may be enhanced by traits, such as phosphate solubilization, and ammonia  
505 production (Yang et al. 2019; Goswami et al. 2013). Several, *Pseudomonas* species poses urease  
506 activity (Goswami et al. 2015) and tolerate, transition metals via the production of extracellular  
507 polysaccharides (EPS), such as Rhamnolipids, that form complexes with heavy metals (Meliani  
508 2015).

509

510 *Alcanivorax* species, a highly abundant recurrent group A microbe, reduced alkane  
511 hydrocarbons, and possessed many enzymes for  $\beta$ -oxidation of fatty acids, the glyoxylate bypass,  
512 and the gluconeogenesis. These gene functions carried by *Alcanivorax* suggest they break down  
513 the complex hydrocarbons and fatty acid rich metabolites and may facilitate other member of the  
514 microbiome by providing simpler metabolic products that can be utilized. They also include  
515 enzymes for synthesis of riboflavin and unsaturated fatty acids and cardiolipin (Sabirova et al.  
516 2020). Cardiolipin is a diphosphatidylglycerol lipid (Schlame, Brody, and Hostetler 1993) and is

517 more highly saturated in sharks than other vertebrates (Shadwick, Farrell, and Brauner 2015) and  
518 sequences similar to Cardiolipin were identified in the metagenomes.

519 *Erythrobacter* species, a highly abundance group A microbe that was negatively correlated with  
520 many other microbes are mostly aerobic anoxygenic phototrophic bacteria, containing  
521 bacteriochlorophyll a, but lack the genes of autotrophic CO<sub>2</sub> fixation pathway, thus  
522 photoheterotrophic metabolism requiring a supply of organic substrates. Several *Erythrobacter*  
523 species have genes encoding enzymes for glycolysis and the tricarboxylic acid cycle but lack  
524 genes for nitrogenase or nitrate reductase thus are reliant on other forms of organic nitrogen  
525 (Koblizek et al. 2003), which matches the lower proportion of sequences identified in the  
526 *Erythrobacter* in the *T. semifasciata* microbiome. *Erythrobacter* carry heavy metal resistance  
527 genes, including resistance to lead, cadmium, zinc, mercury, nickel, cobalt, and arsenicals  
528 (Zheng et al. 2016) and these genes were highly present in the metagenomic profiles. The  
529 behaviour of the leopard sharks, being in shallow water with higher light conditions may have  
530 provided the *Erythrobacter* with a competitive advantage over other microbial groups.

531 The last group A recurrent microbe was *Marinobacter* and these organisms are opportunistic  
532 generalists that switch rapidly between lithoheterotrophy to heterotrophy, in both anaerobic and  
533 aerobic conditions, in response to nutrient pulses. They have fast growth, outgrowing other  
534 species in culture (Handley and Lloyd 2013). *Marinobacter* are able to respire inorganic  
535 compounds that are usually found in metal rich environments (Handley and Lloyd 2013), and we  
536 show they have many genes associated with metal resistance and transport. *Marinobacter* use  
537 many hydrocarbons as a sole energy source, and produce large quantities of bioemulsifier, which  
538 aid in bacterial adhesion to hydrophobic surfaces.

539 The recurrent group B microbes, the opportunists, were negatively correlated with most other  
540 groups and had a high relative abundance of genes associated with carbon metabolism. *Gramella*  
541 species degrades high molecular weight organic matter and encoding hydrolytic enzymes  
542 predicting a preference for polymeric carbon sources and have range of gliding motility that  
543 provide for surface adhesion (Bauer et al. 2006), features that enable the organism to live on the  
544 surface of elasmobranchs. However, these microbes had fewer genes in ammonia assimilation,  
545 promoting their coexistence with the more abundant species. *Leeuwenhoekiella*, a marine  
546 Flavobacteria, has gliding motility, heterotrophic growth, is pigmented and often found in

547 associated with photosynthetic microbes and converts nitroalkanes into nitrite (Tahon et al.  
548 2020). *Alteromonas* are non-phototrophic, heterotrophic, with flexible genome for taking  
549 advantage of influx of nutrients, particularly polymers, and some degrade polycyclic aromatic  
550 hydrocarbons (Math et al. 2012). *Alteromonas* have high flexibility in the metal resistant genes  
551 and efflux pumps and show strain differences in the copper-zinc-cobalt gene (*czc*) cassettes by  
552 successive insertions at a tRNA gene, with the numbers of *czc* cassettes varying from zero to  
553 three (Lopez-Perez et al. 2012) and these highly abundant in this genus in the *T. semifasciata*  
554 microbiome. *Pseudoalteromonas* and *Alteromonas* utilized extracellular hydrolysis as the major  
555 decomposition pathway of peptides and released fragments of amino acids into the surrounding  
556 environment (Liu and Liu 2020) and may have enable them to outcompete *Marinobacter* which  
557 is unable to conduct extracellular hydrolysis processes. However, these free amino acids may be  
558 used by other microbes, such as the non-recurrent group C and D microbes.

559 The group C recurrent microbes, the specialists, had less relative abundance overall but showed  
560 high relative abundance of a few metabolic pathways (Figure 5). *Ruegeria* had a high proportion  
561 of sequences associated with urea metabolism, compared with its relatively low proportional  
562 abundance. *Ruegeria* are able to use Trimethylamine (TMA) and trimethylamine N-oxide  
563 (TMAO) as an energy source to product intracellular ATP (Lidbury, Murrell, and Chen 2015).  
564 TMAO and TMA are used by elasmobranchs for osmoregulation.

565 *Sphingopyxis* also had low relative abundance, utilizing carbon and nitrogen compounds as  
566 substrates for growth but are generally slow growing (Moran et al. 2007). Serine, a pathway that  
567 was overrepresented in *Sphingopyxis*, can serve as a nitrogen source for the growth of some  
568 species, but not as a carbon source (Williams et al. 2009). Ammonia and nitrate are used as  
569 nitrogen sources, but there is a high energetic cost associated with nitrate utilization (Verma et  
570 al. 2020). *Sphingomonas* are closely related to *Sphingoyxis* and both produces  
571 exopolysaccharides (EPS) (Chang et al. 2021). The production of these compounds may provide  
572 biofilm development on the shark skin. Therefore, each recurrent microbial group was providing  
573 a different set of functional genes that enhanced coexistence and reflected the products that may  
574 be associated with shark metabolism and excreted via the mucus.

575 *Gene functions linked to host metabolic processes*

576 The stability of the functional potential of the epidermal microbiome suggests the elasmobranch  
577 physiology and dermal denticle topography are strong drivers of microbiome function, and we  
578 have developed a model to link the microbiome function with shark metabolism (Figure 7).  
579 Elasmobranchs rely on protein as the primary food source and use ketogenic pathways and  
580 produce high ketone bodies and hydrocarbons (Speers-Roesch and Treberg 2010). The functions  
581 that were present in metagenomes suggests that the microbes were responding to the presence of  
582 these compounds in the minimal mucus that covers the sharks. For example, *Alxavorax* and  
583 *Marinobacter* carried the genes to degrade hydrocarbons. There are few descriptions of the  
584 compounds within the mucus of Elasmobranchs, and these included high levels of proteins  
585 (Tsutsui et al., 2009) with moderate to high disulphide concentrations (Meyer et al., 2007a). A  
586 recent transcriptome analysis of the integument of cookie cutter sharks identified  
587 Glyceraldehyde-3-phosphate dehydrogenase and Fructose-bisphosphate aldolase A transcripts,  
588 both play key roles in the glycolysis and gluconeogenesis (Delroisse et al. 2021) suggesting these  
589 products are being produced in the skin and may be available to the microbial community.  
590 Protein metabolism and nitrate and nitrite ammonification, urea decomposition with genes such  
591 as trimethylamine N-oxide (TMAO) reductase were significant functions in the microbiomes.  
592 The low levels of nitrogen fixation in the microbiome and the high proportional abundance of  
593 nitrogen metabolism and urea decomposition and the presences of within the microbiome  
594 suggest the elasmobranch is a nitrogen-rich environment (Hazon et al. 2003; Dowd et al. 2010).  
595 Proteasomes, metallo-carboxypeptidase, aminopeptidase genes, protein degradation and  
596 biosynthesis functional genes suggest a propensity of the microbes for protein degradation. There  
597 was no evidence of dentine, hydrolysate, or collagen degradation in the microbiome, suggesting  
598 that the microbes are not breaking down the dermal denticles, which signifies a lack of negative  
599 impact on the sharks. Therefore, a commensal connection between *T. semifasciata* and the  
600 epidermis microbiome is established through the passive resource subsidization of these  
601 microbiome functions.  
602  
603 Cobalt-zinc-cadmium resistance and ton/to transport genes are highly prevalent functional genes  
604 shared across epidermis microbiomes of *T. semifasciata* (this study), *A. vulpinus* (Doane et al.  
605 2017), *Rhincodon typus* and *Urobatis halleri* (Doane et al. 2020). Elasmobranchs bioaccumulate  
606 heavy metals and shunt these compounds to the epidermis (Escobar-Sanchez, Galvan-Magana,

607 and Rosiles-Martinez 2010; Maz-Courrau et al. 2012), and the epidermal microbiomes are  
608 responding to the presence of these compounds. The prevalence of heavy metal resistance genes  
609 may provide a biomarker of elasmobranchs health and identify those exposed to anthropogenic  
610 sources of heavy metals in the environment providing an early warning sign of declining health.

611

## 612 **Conclusions**

613 The highly structured epidermis of elasmobranchs, in this case, *T. semifasciata*, promotes a  
614 diverse microbiome that has a flexible taxonomic makeup where many genera coexist. The  
615 microbial community was maintained by functional redundancy driven by the taxonomic  
616 flexibility and various microbes "flip-flopping" in abundance with one another, which kept the  
617 microbial niches filled across the years. The high relative abundance of genes involved in  
618 nitrification and denitrification, urea decomposition, and heavy metal resistance genes in the  
619 epidermis microbiome across all *T. semifasciata* individuals suggests a connection with the host  
620 metabolism potentially through passive subsidization of organic nitrogen, proteins,  
621 hydrocarbons, and heavy metals.

622

623 **Abbreviations**

624 Not applicable

625

626 **Ethical Approval and Consent to participate**

627 Animal handling and ethics were reviewed at San Diego State University through IACUC under  
628 permit APF #14-05-011D, APF #17-11-010D, APF # 18-05-007D. Sampling was conducting  
629 under state permit SCP #12847 and SCP #9893 from the California Department of Fish and  
630 Wildlife.

631

632 **Consent for publication**

633 Not applicable

634

635 **Availability of data and materials**

636 All data will be publicly released upon publication.

637

638 **Competing interests**

639 The authors declare no conflict of interest.

640

641 **Funding**

642 We acknowledge support from S. Lo and B. Billings. We acknowledge funding support from  
643 NSF Division of Undergraduate Education # 1323809 and NSF Division of Molecular and  
644 Cellular Science # 1330800.

645

646 **Author's contribution**

647 MD collected all field samples, constructed the ideas and help write the paper, CJ analyzed the  
648 data and wrote the manuscript, EK, AT, AG, SJ, captured and prepared samples and provide  
649 feedback on the manuscript, MMM and LL provided sequencing and analysis, AN facilitated the  
650 catching of leopard sharks, RD provided the illustration, ED conceptualized the idea, analyzed,  
651 wrote and lead the project.

652

653 **Acknowledgements**

654 We would like to thank the students in the SDSU undergraduate Ecological Metagenomic class  
655 assisting with the processing and sequencing of the leopard shark metagenomes.

656

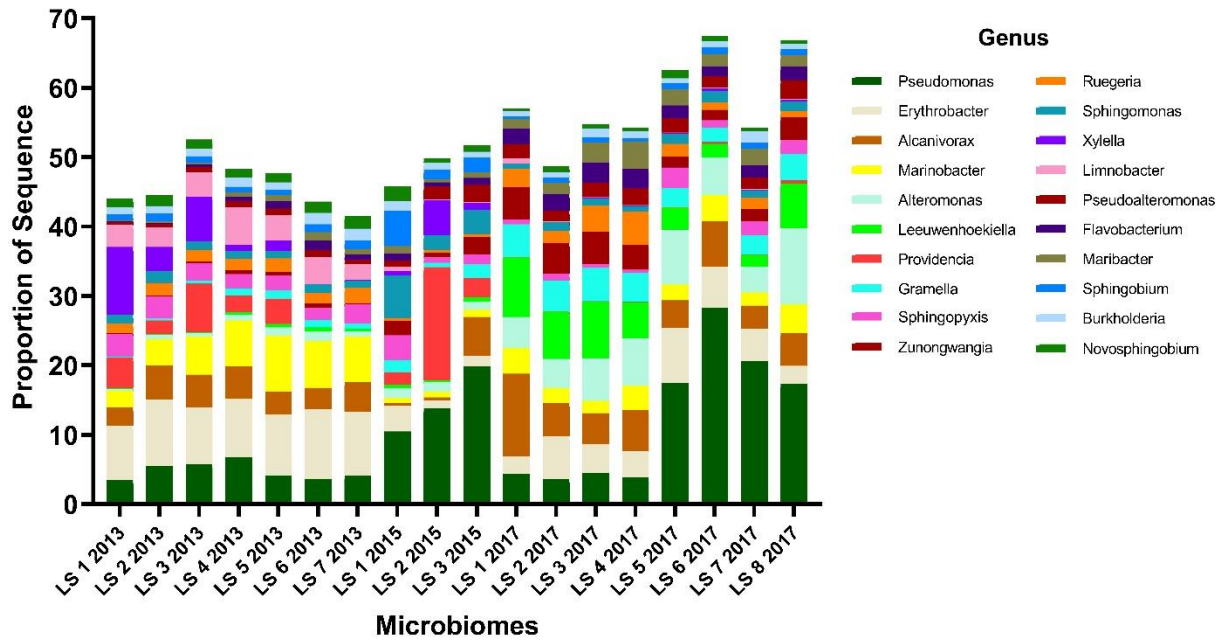
657 **Authors' information**

658 <sup>1</sup>College of Science and Engineering, Flinders University, Bedford Park, South Australia,  
659 Australia; <sup>2</sup>Department of Biology, San Diego State University, San Diego, California, USA;  
660 <sup>3</sup>Hopkins Marine Station, Stanford University, Pacific Grove, California, USA; <sup>4</sup>Laurence  
661 Livermore National Labs, Livermore, California, USA; <sup>5</sup>Australian Centre for Ecogenomics,  
662 University of Queensland, St Lucia, Queensland, Australia; <sup>6</sup>Department of Environmental and  
663 Ocean Sciences, University of San Diego, San Diego, California, USA; <sup>7</sup>Scripps Institution of  
664 Oceanography, University of California – San Diego, La Jolla, California, USA

665

666  
667  
668  
669

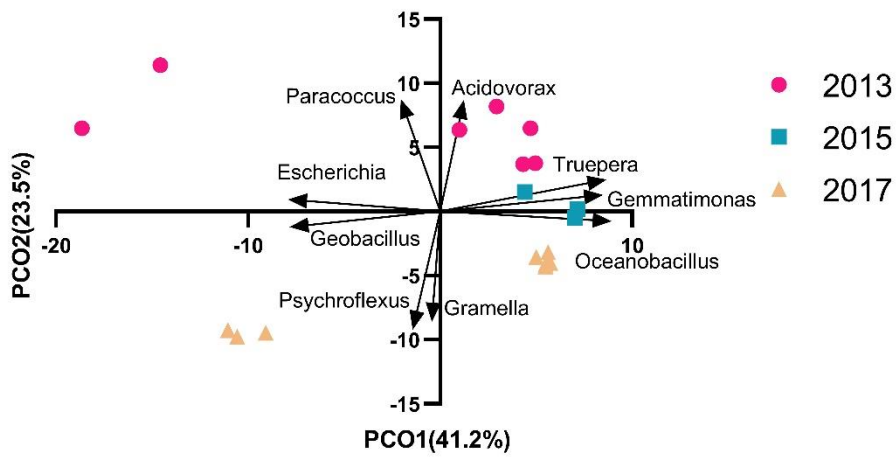
Tables and Figures



670  
671  
672  
673

Figure 1. The relative proportions of the most abundant microbial genera represented in the *Triakis semifasciata* microbiome across four years.

674



675

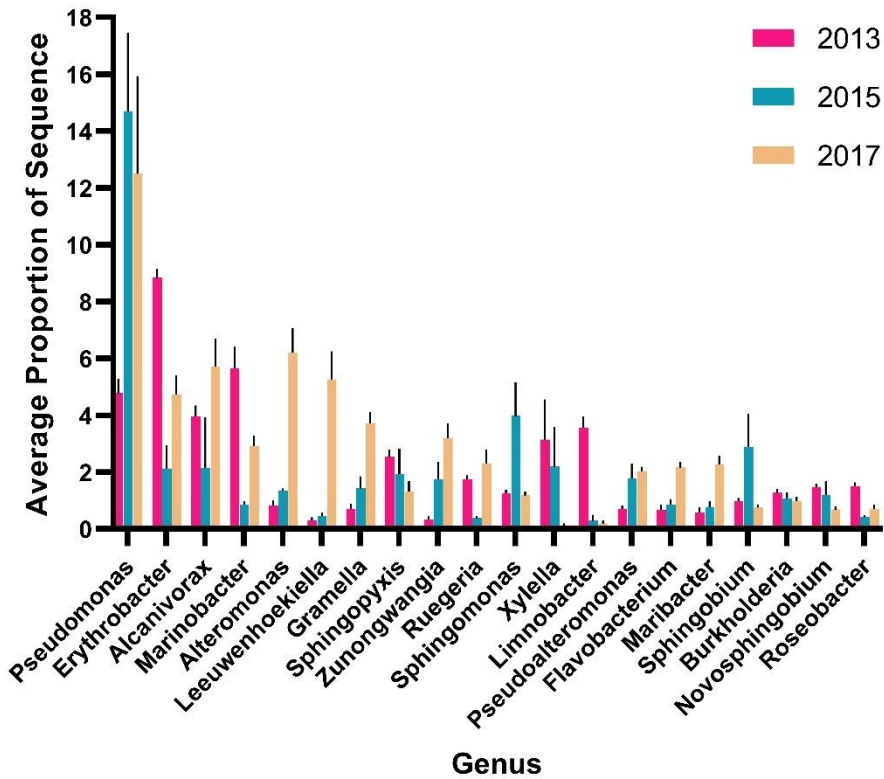
676

677 Figure 2 The microbial genera of the *Triakis semifasciata* epidermal microbiome clustered by year, with a  
678 few outliers on the principal component analysis conducted on proportional sequence distribution.

679

680

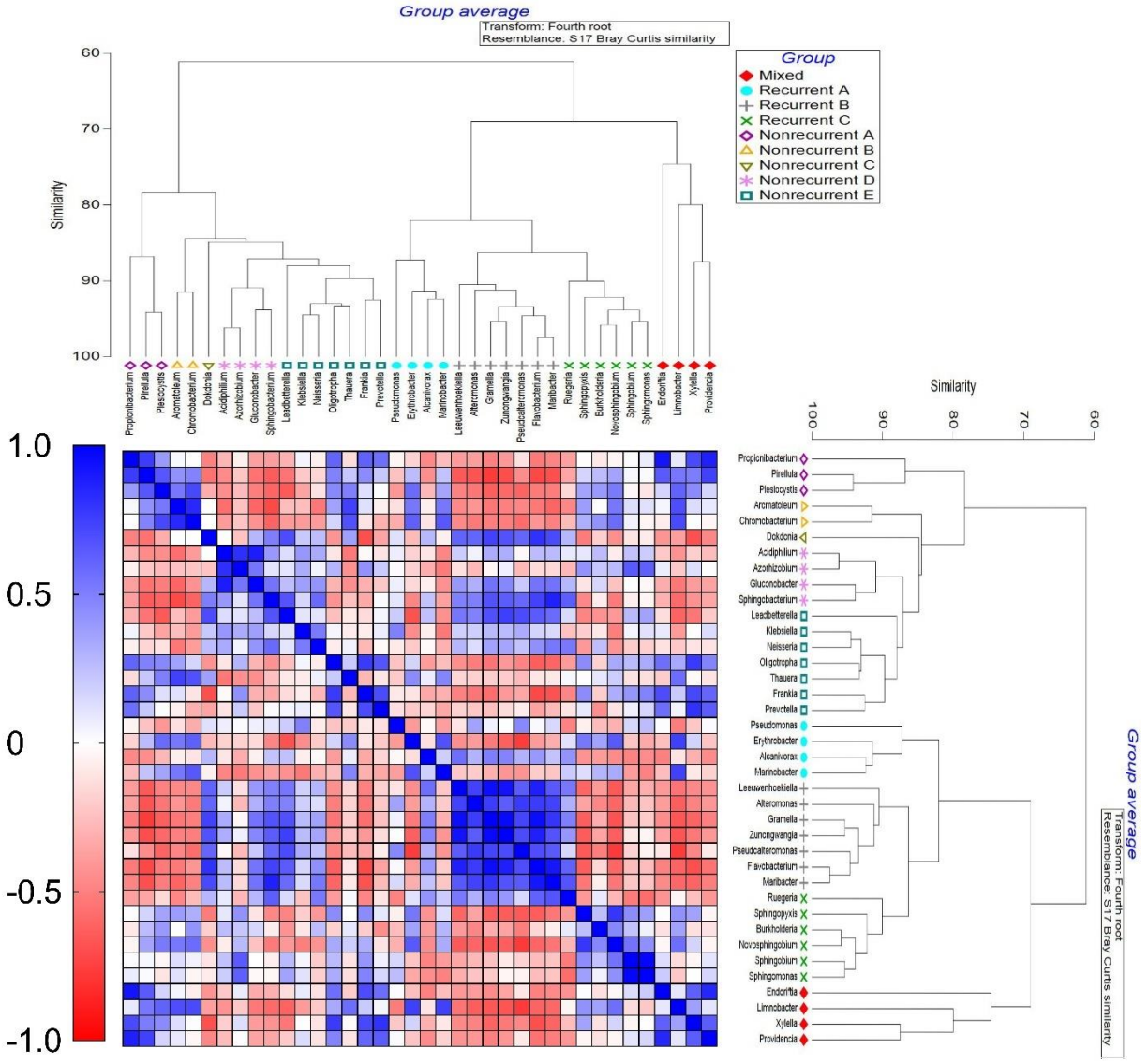
681



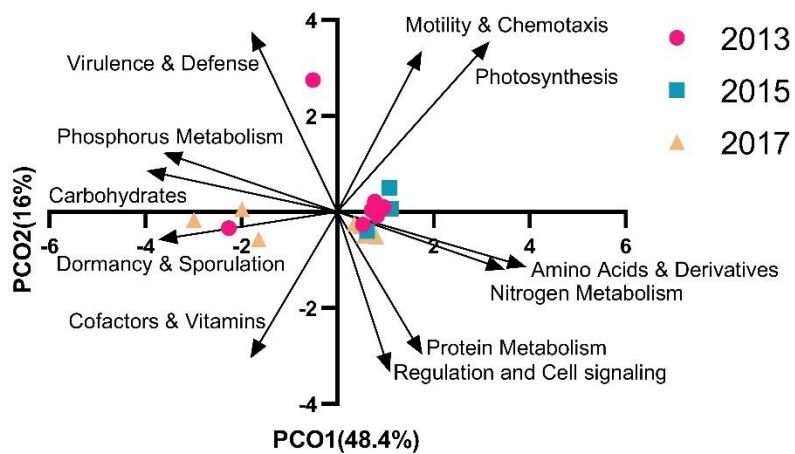
682

683 Figure 3. The mean relative abundance ( $\pm$  S.E.) of abundant recurrent genera per year on the *Triakis*  
684 *semifasciata* epidermal microbiome, showing flexibility with no abundant genera becoming extinct over  
685 the four years.

686



687  
 688 Figure 4. Positive and negative correlations occurred between most abundant 19 recurrent and non-  
 689 recurrent microbes in the *Triakis semifasciata* epidermal microbiome. Bray Curtis similarity was used to  
 690 cluster the genera with similar proportional abundance across years and the relationship with other genera  
 691 was compared using a Pearson's correlation, displayed as a heat map where red is a negative correlation  
 692 and blue is a positive correlation.  
 693  
 694



695

696

697 Figure 5. The functional potential of the *Triakis semifasciata* epidermal microbiome was stable across the  
 698 four-year period, shown using a principal component analysis.

699

700

701

702

703

704

705

706

707

708

709

710

711

712

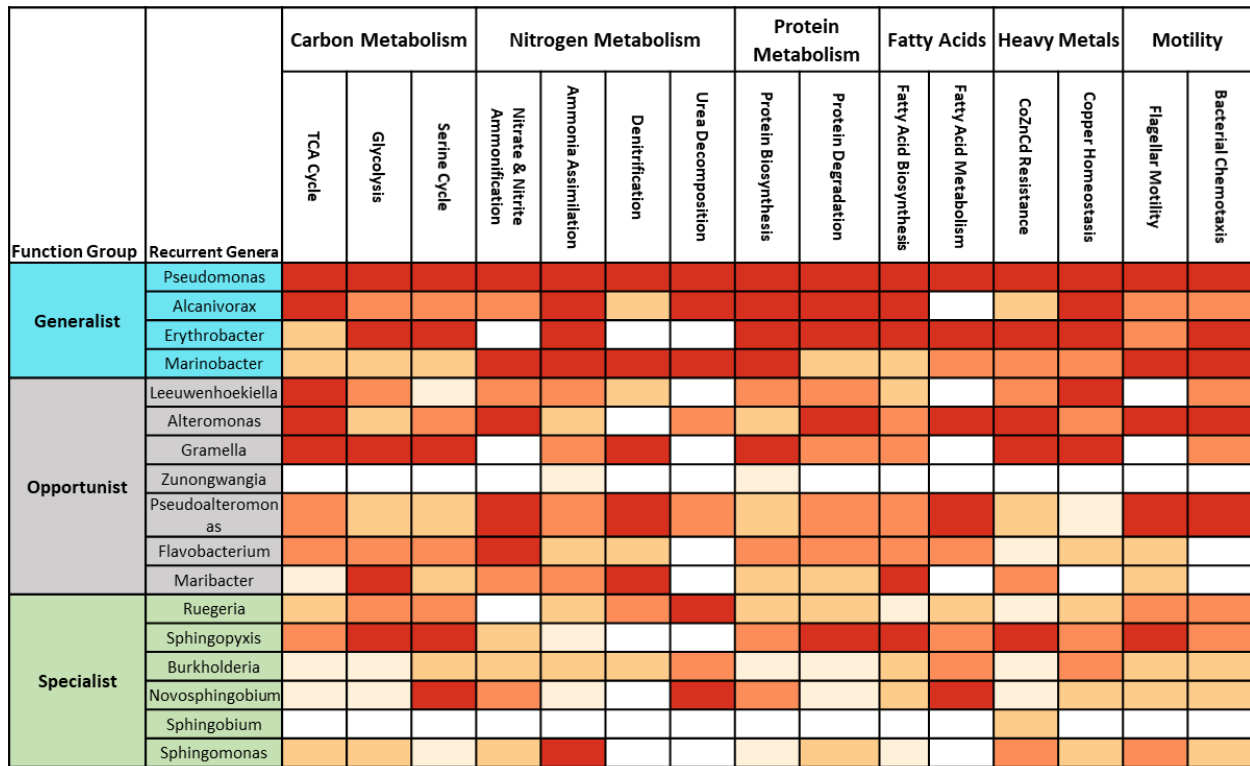
713

714

715

716

717



718

719

720

721

722

723

724

725

726

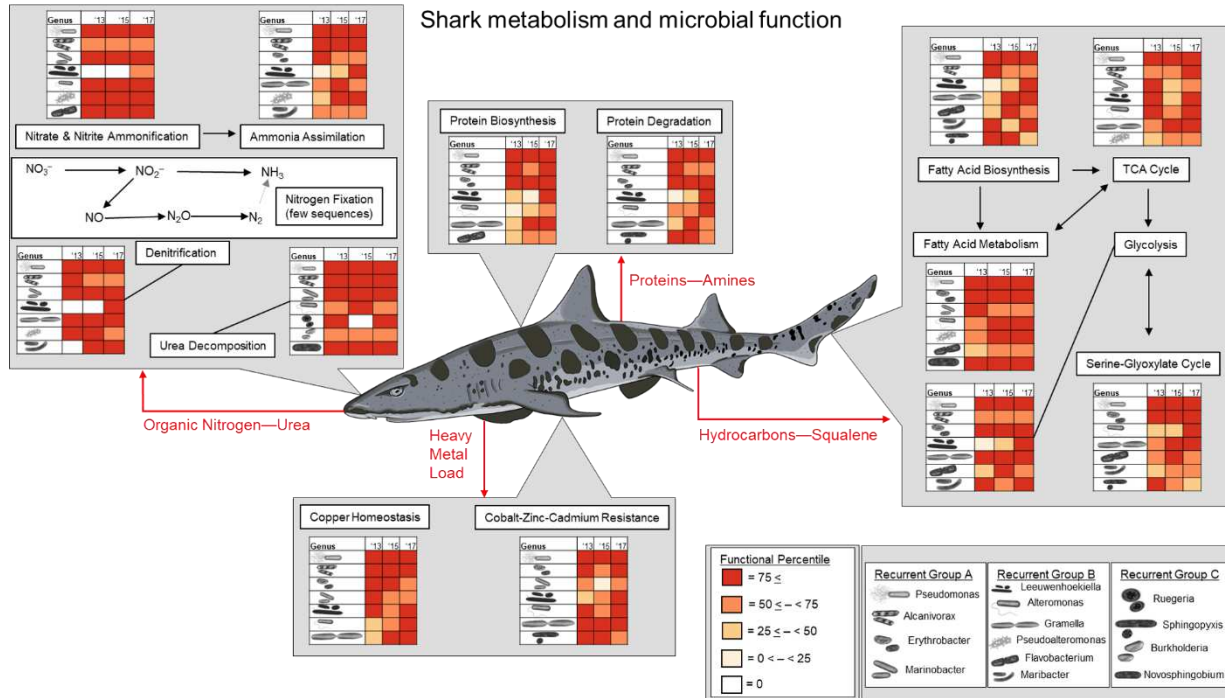
727

728

729

730

Figure 6. Heat map of the mean proportion of genes associated with each metabolism in the 17 most abundant recurrent taxon in group A (aqua), group B(grey) and group c (green), shows genes were mostly shared across taxon, but some specialization occurred. The proportion of sequences were divided into quartiles, where darker colors represent higher percentile (>75– dark red, 50-75 orange/red, 25-50 - orange, and 0-25 - pale orange). No color represented no sequences for that metabolism held by that genus.



731  
 732  
 733  
 734  
 735  
 736  
 737  
 738  
 739  
 740  
 741

Figure 7. The links between the functional potential of the *Triakis semifasciata* epidermal microbiome and the host metabolism. The proportion of each gene in each taxon were identified and classed into quartiles. Most taxa had most functions suggesting the microbiome displays weak competition and is responding to the metabolic processes of the host.

742 Table 1. The *Triakis semifasciata* metagenome statistics, including collection date, total sequences and  
 743 proportion of the metagenome that was annotated by the database.

Metagenome Name	Date	Location	SRA#	Number of sequences	Annotated proteins (%)
LS 1 2013	2013	La Jolla		1188249	20.69
LS 2 2013	2013	La Jolla		1060680	24.36
LS 3 2013	2013	La Jolla		1024296	20.16
LS 4 2013	2013	La Jolla		1154296	21.33
LS 5 2013	2013	La Jolla		2347886	19.79
LS 6 2013	2013	La Jolla		3346424	18.84
LS 7 2013	2013	La Jolla		2330953	20.36
LS 1 2015	2015	La Jolla		1143301	22.68
LS 2 2015	2015	La Jolla		2012275	15.87
LS 3 2015	2015	La Jolla		1635251	20.4
LS 1 2017	2017	La Jolla		701418	75.63
LS 2 2017	2017	La Jolla		898767	74.86
LS 3 2017	2017	La Jolla		636435	46.71
LS 4 2017	2017	La Jolla		324102	68.57
LS 5 2017	2017	La Jolla		312135	61.76
LS 6 2017	2017	La Jolla		693318	43.43
LS 7 2017	2017	La Jolla		613946	62.52
LS 8 2017	2017	La Jolla		1189453	43.69

744

745

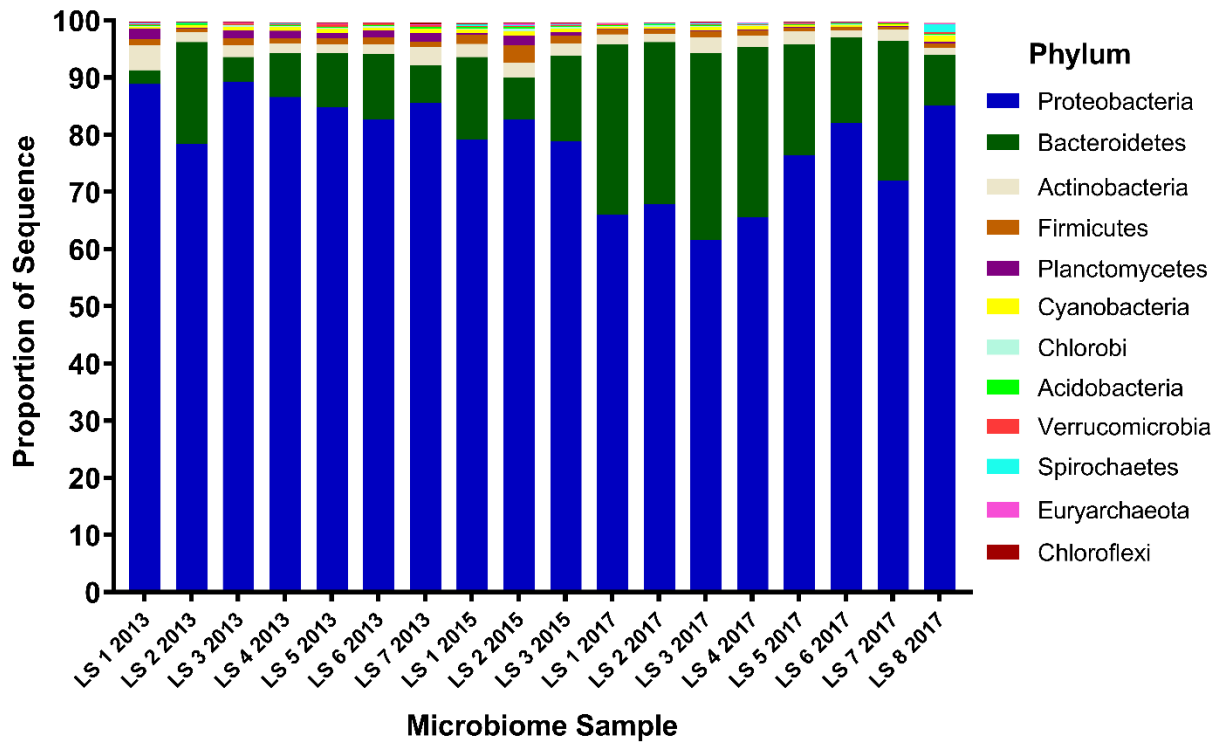
746 Table 2. The genera that contributed to the flexibility in the *Triakis semifasciata* epidermal  
 747 microbiome across four years, calculated via a Simper analysis, with dissimilarity coefficient of  
 748 16.95 between 2013 & 2015; 19.71 for 2013 & 2017; and 15.32 for 2015 & 2017  
 749

Years compared	Phyla	Class	Genus	Percent Contribution
2013 vs 2015	Proteobacteria	Gammaproteobacteria	<i>Providencia</i>	0.9
			<i>Endorifia</i>	0.86
			<i>Marinobacter</i>	0.72
			<i>Pseudomonas</i>	0.61
			<i>Xylella</i>	0.58
		Betaproteobacteria	<i>Alcanivorax</i>	0.58
			<i>Limnobacter</i>	0.87
		Alphaproteobacteria	<i>Erythrobacter</i>	0.7
			<i>Hyphomonas</i>	0.56
			<i>Oceanibulbus</i>	0.66
2013 vs 2017	Bacteroidetes	Flavobacteria	<i>Leeuwenkoekiella</i>	0.9
			<i>Zuongwangia</i>	0.7
			<i>Gramella</i>	0.58
	Proteobacteria	Betaproteobacteria	<i>Limnobacter</i>	0.89
			Gammaproteobacteria	<i>Providencia</i>
		<i>Alteromonas</i>		0.73
		<i>Xylella</i>		0.67
		Alphaproteobacteria	<i>Endorifia</i>	0.54
			<i>Hyphomonas</i>	0.48
		Planctomycetia	<i>Planctomyces</i>	0.47
2015 vs 2017	Proteobacteria	Gammaproteobacteria	<i>Providencia</i>	1.41
			<i>Endorifia</i>	1.11
			<i>Psychrobacter</i>	0.91
			<i>Xylella</i>	0.81
			<i>Alcanivorax</i>	0.75
		Alteromonas	<i>Alteromonas</i>	0.69
			<i>Pseudomonas</i>	0.52
		Alphaproteobacteria	<i>Ruegeria</i>	0.59
			Betaproteobacteria	<i>Achromobacter</i>
		Bacteroidetes	Flavobacteria	<i>Leeuwenkoekiella</i>

750

751

752 **Supplementary material**

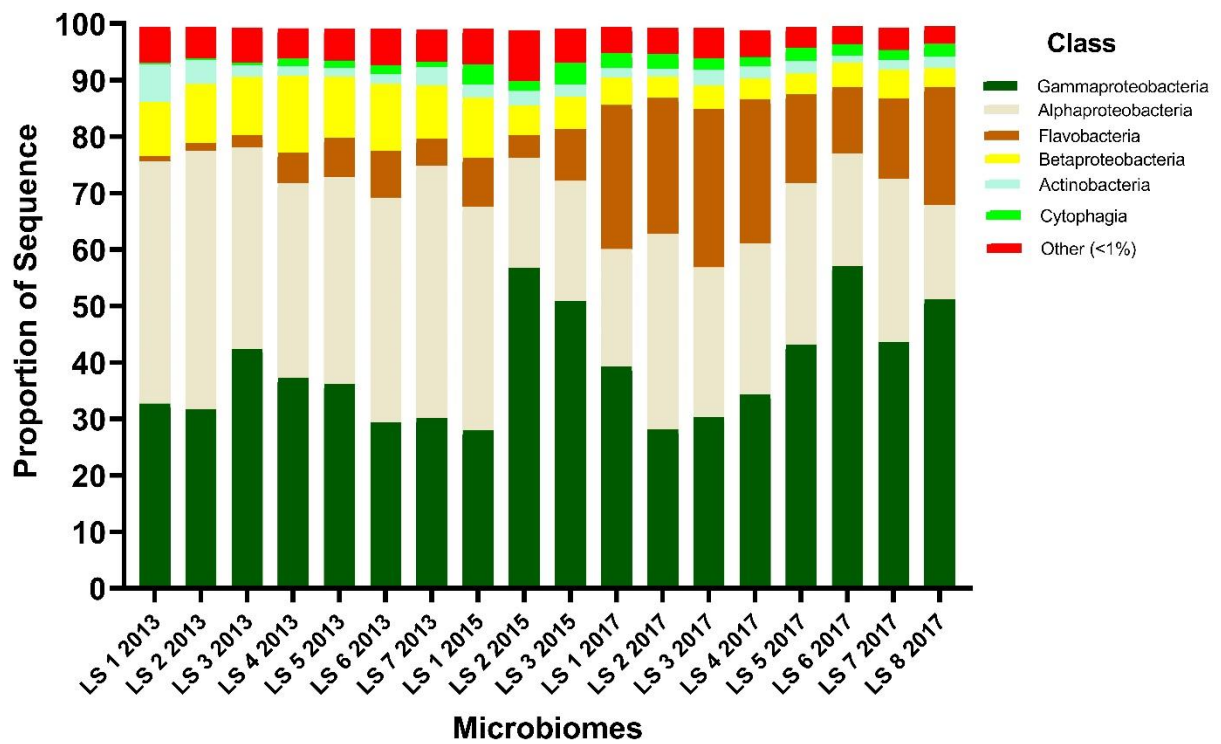


753

754

755 Supplementary Figure 1. The phylum profile of the *Triakis semifasciata* epidermal microbiome had

756 stable across four years.



757

758

759 Supplementary Figure 2.

760 The relative distribution of microbial classes in the *Triakis semifasciata* microbiome were similar over a

761 four-years.

762

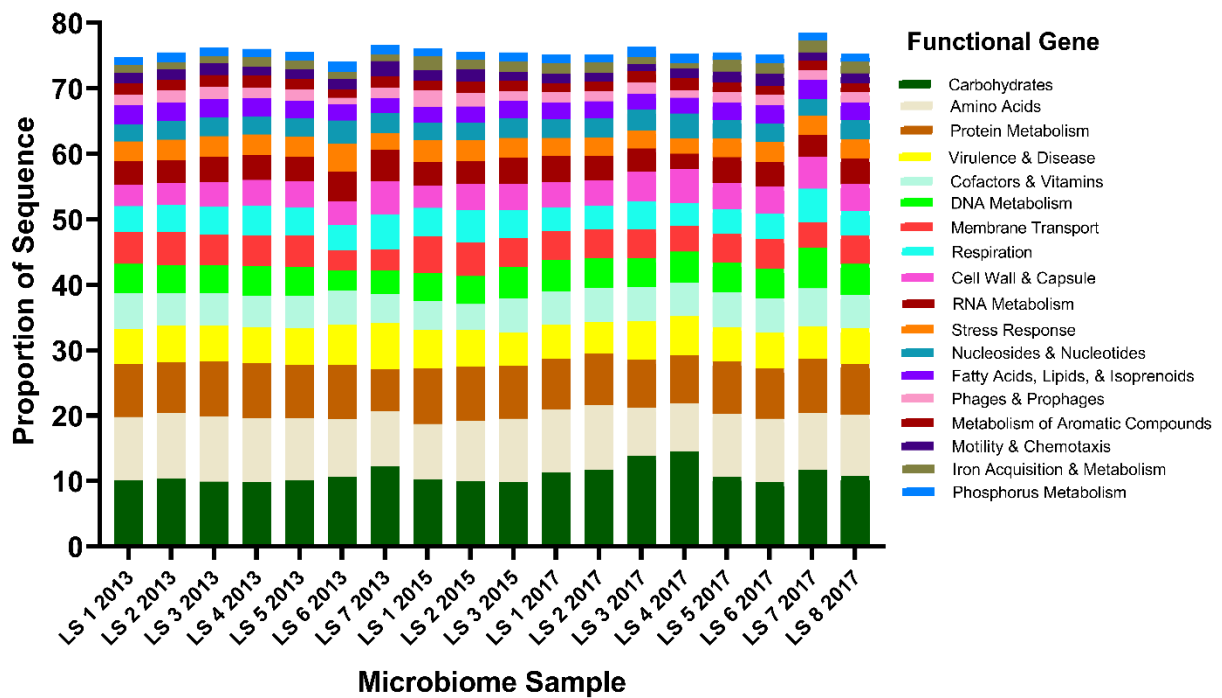
763

764

765

766

767



768

769 Supplementary Figure 3. The major metabolisms identifying within the *Triakis semifasciata*  
 770 microbiomes.

771

772 **References**

773 Anderson, M. J. 2017. 'Permutational multivariate analysis of variance (PERMANOVA).' in T. Colton N.  
 774 Balakrishnan, B. Everitt, W. Piegorisch, F. Ruggeri, and J. Teugels (ed.), *Wiley statsref: statistics*  
 775 *reference online* (John Wiley and Sons: Hoboken, NJ, USA. ).

776 Anderson, M.J. 2006. 'Distance-based tests for homogeneity of multivariate dispersions. ', *Biometrics*,,  
 777 62: 245–53.

778 Aziz, R. K., D. Bartels, A. A. Best, M. DeJongh, T. Disz, R. A. Edwards, K. Formsma, S. Gerdes, E. M. Glass,  
 779 M. Kubal, F. Meyer, G. J. Olsen, R. Olson, A. L. Osterman, R. A. Overbeek, L. K. McNeil, D.  
 780 Paarmann, T. Paczian, B. Parrello, G. D. Pusch, C. Reich, R. Stevens, O. Vassieva, V. Vonstein, A.  
 781 Wilke, and O. Zagnitko. 2008. 'The RAST server: Rapid annotations using subsystems  
 782 technology', *Bmc Genomics*, 9.

783 Ballantyne, J. S. 1997. ' Jaws: the inside story. The metabolism of elasmobranch fishes. ', *Comparative*  
 784 *Biochemistry and Physiology Part B: Biochemistry and Molecular Biology* . 118: 703-42.

785 Bauer, M., M. Kube, H. Teeling, M. Richter, T. Lombardot, E. Allers, C. A. Wurdemann, C. Quast, H. Kuhl,  
 786 F. Knaust, D. Wobken, K. Bischof, M. Mussmann, J. V. Choudhuri, F. Meyer, R. Reinhardt, R. I.  
 787 Amann, and F. O. Glockner. 2006. 'Whole genome analysis of the marine Bacteroidetes'Gramella  
 788 forsetii' reveals adaptations to degradation of polymeric organic matter', *Environmental*  
 789 *Microbiology*, 8: 2201-13.

790 Bierlich, K. C., C. Miller, E. DeForce, A. S. Friedlaender, D. W. Johnston, and A. Apprill. 2018. 'Temporal  
 791 and Regional Variability in the Skin Microbiome of Humpback Whales along the Western  
 792 Antarctic Peninsula', *Appl Environ Microbiol*, 84.

793 Cantu, V. A., J. Sadural, and RA Edwards. 2019. 'PRINSEQ ++, a multi-threaded tool for fast and efficient  
794 quality control and preprocessing of sequencing datasets.', *PeerJ Preprints*, 7: 43–45.

795 Chang, A. P., J. Qian, H. Li, Y. L. Wang, J. Y. Lin, Q. M. He, Y. L. Shen, and H. Zhu. 2021. 'Characterization  
796 and Function of a Novel Welan Gum Lyase From Marine Sphingomonas sp. WG', *Frontiers in*  
797 *Microbiology*, 12: 638355.

798 Chien, H. W., X. Y. Chen, W. P. Tsai, and M. Lee. 2020. 'Inhibition of biofilm formation by rough shark  
799 skin-patterned surfaces', *Colloids and Surfaces B-Biointerfaces*, 186.

800 Clarke, K. R., P. J. Somerfield, and R. N. Gorley. 2008. 'Testing of null hypotheses in exploratory  
801 community analyses: similarity profiles and biota-environment linkage', *Journal of Experimental*  
802 *Marine Biology and Ecology*, 366: 56-69.

803 ———. 2016. 'Clustering in non-parametric multivariate analyses', *Journal of Experimental Marine*  
804 *Biology and Ecology*, 483: 147-55.

805 Costello, E. K., K. Stagaman, L. Dethlefsen, B. J. Bohannan, and D. A. Relman. 2012. 'The application of  
806 ecological theory toward an understanding of the human microbiome', *Science*, 336: 1255-62.

807 Delroisse, J., L. Duchatelet, P. Flammang, and J. Mallefet. 2021. 'Photophore Distribution and Enzymatic  
808 Diversity Within the Photogenic Integument of the Cookie-Cutter Shark *Isistius brasiliensis*  
809 (*Chondrichthyes: Dalatiidae*)', *Frontiers in Marine Science*, 8.

810 Dillon, E. M., R. D. Norris, and A. O'Dea. 2017. 'Dermal denticles as a tool to reconstruct shark  
811 communities', *Marine Ecology Progress Series*, 566: 117-34.

812 Dinsdale, E. A., R. A. Edwards, D. Hall, F. Angly, M. Breitbart, J. M. Brulc, M. Furlan, C. Desnues, M.  
813 Haynes, L. L. Li, L. McDaniel, M. A. Moran, K. E. Nelson, C. Nilsson, R. Olson, J. Paul, B. R. Brito, Y.  
814 J. Ruan, B. K. Swan, R. Stevens, D. L. Valentine, R. V. Thurber, L. Wegley, B. A. White, and F.  
815 Rohwer. 2008. 'Functional metagenomic profiling of nine biomes', *Nature*, 452: 629-U8.

816 Dinsdale, E. A., O. Pantos, S. Smriga, R. A. Edwards, F. Angly, L. Wegley, M. Hatay, D. Hall, E. Brown, M.  
817 Haynes, L. Krause, E. Sala, S. A. Sandin, R. V. Thurber, B. L. Willis, F. Azam, N. Knowlton, and F.  
818 Rohwer. 2008. 'Microbial ecology of four coral atolls in the Northern Line Islands', *Plos One*, 3:  
819 e1584.

820 Doane, M. P., J. M. Haggerty, D. Kacev, B. Papudeshi, and E. A. Dinsdale. 2017. 'The skin microbiome of  
821 the common thresher shark (*Alopias vulpinus*) has low taxonomic and gene function -diversity',  
822 *Environmental Microbiology Reports*, 9: 357-73.

823 Doane, M. P., D. Kacev, S. Harrington, K. Levi, D. Pande, A. Vega, and E. A. Dinsdale. 2018. 'Mitochondrial  
824 recovery from shotgun metagenome sequencing enabling phylogenetic analysis of the common  
825 thresher shark (*Alopias vulpinus*)', *Meta Gene*, 15: 10-15.

826 Doane, M. P., M. M. Morris, B. Papudeshi, L. Allen, D. Pande, J. M. Haggerty, S. Johri, A. C. Turnlund, M.  
827 Peterson, D. Kacev, A. Nosal, D. Ramirez, K. Hovel, J. Ledbetter, A. Alker, J. Avalos, K. Baker, S.  
828 Bhide, E. Billings, S. Byrum, M. Clemens, A. J. Demery, L. F. O. Lima, O. Gomez, O. Gutierrez, S.  
829 Hinton, D. Kieu, A. Kim, R. Loaiza, A. Martinez, J. McGhee, K. Nguyen, S. Parlan, A. Pham, R.  
830 Price-Waldman, R. A. Edwards, and E. A. Dinsdale. 2020. 'The skin microbiome of elasmobranchs  
831 follows phylosymbiosis, but in teleost fishes, the microbiomes converge', *Microbiome*, 8.

832 Dowd, W. W., B. N. Harris, J. J. Cech, Jr., and D. Kultz. 2010. 'Proteomic and physiological responses of  
833 leopard sharks (*Triakis semifasciata*) to salinity change', *Journal of Experimental Biology*, 213:  
834 210-24.

835 Egan, S., and M. Gardiner. 2016. 'Microbial Dysbiosis: Rethinking Disease in Marine Ecosystems',  
836 *Frontiers in Microbiology*, 7: 991.

837 Escobar-Sanchez, O., F. Galvan-Magana, and R. Rosiles-Martinez. 2010. 'Mercury and selenium  
838 bioaccumulation in the smooth hammerhead shark, *Sphyrna zygaena* Linnaeus, from the  
839 Mexican Pacific Ocean', *Bull Environ Contam Toxicol*, 84: 488-91.

840 Goswami, D., K. Patel, S. Parmar, H. Vaghela, N Muley, P Dhandhukia, and J.N. Thakker. 2015.  
841 'Elucidating multifaceted urease producing marine *Pseudomonas aeruginosa* BG as a cogent  
842 PGPR and bio-control agent.', *Plant Growth Regulation*, 75: 253–63.

843 Goswami, D., H. Vaghela, S. Parmar, P Dhandhukia, and J. Thakker. 2013. 'Plant growth promoting  
844 potentials of *Pseudomonas* spp. strain OG isolated from marine water.', *J Plant Interact*, 8: 281–  
845 90.

846 Guo, H., C. Chen, and D. J. Lee. 2019. 'Nitrogen and sulfur metabolisms of *Pseudomonas* sp. C27 under  
847 mixotrophic growth condition', *Bioresour Technol*, 293: 122169.

848 Handley, K. M., and J. R. Lloyd. 2013. 'Biogeochemical implications of the ubiquitous colonization of  
849 marine habitats and redox gradients by *Marinobacter* species', *Frontiers in Microbiology*, 4.

850 Hazon, N., A. Wells, R. D. Pillans, J. P. Good, W. Gary Anderson, and C. E. Franklin. 2003. 'Urea based  
851 osmoregulation and endocrine control in elasmobranch fish with special reference to  
852 euryhalinity', *Comp Biochem Physiol B Biochem Mol Biol*, 136: 685-700.

853 Johri, S., M. P. Doane, L. Allen, and E. A. Dinsdale. 2019. 'Taking Advantage of the Genomics Revolution  
854 for Monitoring and Conservation of Chondrichthyan Populations', *Diversity-Basel*, 11.

855 Kanehisa, M., S. Goto, Y. Sato, M. Furumichi, and M. Tanabe. 2012. 'KEGG for integration and  
856 interpretation of large-scale molecular data sets', *Nucleic Acids Research*, 40: D109-D14.

857 Kanehisa, M., Y. Sato, M. Kawashima, M. Furumichi, and M. Tanabe. 2016. 'KEGG as a reference  
858 resource for gene and protein annotation', *Nucleic Acids Research*, 44: D457-D62.

859 Kim, M., S. Lee, H. D. Park, S. I. Choi, and S. Hong. 2012. 'Biofouling control by quorum sensing inhibition  
860 and its dependence on membrane surface', *Water Science and Technology*, 66: 1424-30.

861 Kimes, N. E., W. R. Johnson, M. Torralba, K. E. Nelson, E. Weil, and P. J. Morris. 2013. 'The *Montastraea*  
862 *faveolata* microbiome: ecological and temporal influences on a Caribbean reef-building coral in  
863 decline', *Environmental Microbiology*, 15: 2082-94.

864 Koblizek, M., O. Beja, R. R. Bidigare, S. Christensen, B. Benitez-Nelson, C. Vetriani, M. K. Kolber, P. G.  
865 Falkowski, and Z. S. Kolber. 2003. 'Isolation and characterization of *Erythrobacter* sp strains from  
866 the upper ocean', *Archives of Microbiology*, 180: 327-38.

867 Lang, Amy. 2020. 'The speedy secret of shark skin', *Physics Today*, 73: 58-59.

868 Lidbury, I. D., J. C. Murrell, and Y. Chen. 2015. 'Trimethylamine and trimethylamine N-oxide are  
869 supplementary energy sources for a marine heterotrophic bacterium: implications for marine  
870 carbon and nitrogen cycling', *Isme Journal*, 9: 760-9.

871 Lima, L. F. O., M. Weissman, M. Reed, B. Papudeshi, A. T. Alker, M. M. Morris, R. A. Edwards, S. J. de  
872 Putron, N. K. Vaidya, and E. A. Dinsdale. 2020. 'Modeling of the Coral Microbiome: the Influence  
873 of Temperature and Microbial Network', *Mbio*, 11.

874 Lima, N., T. Rogers, K. Acevedo-Whitehouse, and MV. Brown. 2012. 'Temporal stability and species  
875 specificity in bacteria associated with the bottlenose dolphins respiratory system.', *Environ*  
876 *Microbiol Rep.*, 4: 89–96.

877 Liu, S., and Z. Liu. 2020. 'Distinct capabilities of different Gammaproteobacterial strains on utilizing small  
878 peptides in seawater', *Sci Rep*, 10: 464.

879 Lopez-Perez, M., A. Gonzaga, A. B. Martin-Cuadrado, O. Onyshchenko, A. Ghavidel, R. Ghai, and F.  
880 Rodriguez-Valera. 2012. 'Genomes of surface isolates of *Alteromonas macleodii*: the life of a  
881 widespread marine opportunistic copiotroph', *Sci Rep*, 2: 696.

882 Lowery, N. V., and T. Ursell. 2019. 'Structured environments fundamentally alter dynamics and stability  
883 of ecological communities', *Proceedings of the National Academy of Sciences of the United*  
884 *States of America*, 116: 379-88.

885 Lynch, J. B., and E. Y. Hsiao. 2019. 'Microbiomes as sources of emergent host phenotypes', *Science*, 365:  
886 1405-08.

887 Magoc, T., and S. L. Salzberg. 2011. 'FLASH: fast length adjustment of short reads to improve genome  
888 assemblies', *Bioinformatics*, 27: 2957-63.

889 Math, R. K., H. M. Jin, J. M. Kim, Y. Hahn, W. Park, E. L. Madsen, and C. O. Jeon. 2012. 'Comparative  
890 genomics reveals adaptation by *Alteromonas* sp. SN2 to marine tidal-flat conditions: cold  
891 tolerance and aromatic hydrocarbon metabolism', *Plos One*, 7: e35784.

892 Maz-Courrau, A., C. Lopez-Vera, F. Galvan-Magana, O. Escobar-Sanchez, R. Rosiles-Martinez, and A.  
893 Sanjuan-Munoz. 2012. 'Bioaccumulation and biomagnification of total mercury in four exploited  
894 shark species in the Baja California Peninsula, Mexico', *Bull Environ Contam Toxicol*, 88: 129-34.

895 Meliani, A. 2015. 'Bioremediation Strategies Employed by *Pseudomonas* Species. .' in Maheshwari D.  
896 (ed.), *Bacterial Metabolites in Sustainable Agroecosystem. Sustainable Development and*  
897 *Biodiversity* (Springer,).

898 Meyer, F., D. Paarmann, M. D'Souza, R. Olson, E. M. Glass, M. Kubal, T. Paczian, A. Rodriguez, R. Stevens,  
899 A. Wilke, J. Wilkening, and R. A. Edwards. 2008. 'The metagenomics RAST server - a public  
900 resource for the automatic phylogenetic and functional analysis of metagenomes', *BMC*  
901 *Bioinformatics*, 9.

902 Meyer, W., and U. Seegers. 2012. 'Basics of skin structure and function in elasmobranchs: a review',  
903 *Journal of Fish Biology*, 80: 1940-67.

904 Meyer, W., U. Seegers, and R. Stelzer. 2007. 'Sulphur, thiols, and disulphides in the fish epidermis, with  
905 remarks on keratinization', *Journal of Fish Biology*, 71: 1135-44.

906 Moran, M. A., R. Belas, M. A. Schell, J. M. Gonzalez, F. Sun, S. Sun, B. J. Binder, J. Edmonds, W. Ye, B.  
907 Orcutt, E. C. Howard, C. Meile, W. Palefsky, A. Goesmann, Q. Ren, I. Paulsen, L. E. Ulrich, L. S.  
908 Thompson, E. Saunders, and A. Buchan. 2007. 'Ecological genomics of marine Roseobacters',  
909 *Appl Environ Microbiol*, 73: 4559-69.

910 Nosal, A. P., A. Caillat, E. K. Kisfaludy, M. A. Royer, and N. C. Wegner. 2014. 'Aggregation behavior and  
911 seasonal philopatry in male and female leopard sharks *Triakis semifasciata* along the open coast  
912 of southern California, USA', *Marine Ecology Progress Series*, 499: 157-75.

913 Nosal, A. P., D. C. Cartamil, J. W. Long, M. Luhrmann, N. C. Wegner, and J. B. Graham. 2013.  
914 'Demography and movement patterns of leopard sharks (*Triakis semifasciata*) aggregating near  
915 the head of a submarine canyon along the open coast of southern California, USA',  
916 *Environmental Biology of Fishes*, 96: 865-78.

917 Ondov, B. D., N. H. Bergman, and A. M. Phillippy. 2011. 'Interactive metagenomic visualization in a Web  
918 browser', *BMC Bioinformatics*, 12: 385.

919 Overbeek, R., T. Begley, R. M. Butler, J. V. Choudhuri, H. Y. Chuang, M. Cohoon, V. de Crecy-Lagard, N.  
920 Diaz, T. Disz, R. Edwards, M. Fonstein, E. D. Frank, S. Gerdes, E. M. Glass, A. Goesmann, A.  
921 Hanson, D. Iwata-Reuyl, R. Jensen, N. Jamshidi, L. Krause, M. Kubal, N. Larsen, B. Linke, A. C.  
922 McHardy, F. Meyer, H. Neuweger, G. Olsen, R. Olson, A. Osterman, V. Portnoy, G. D. Pusch, D. A.  
923 Rodionov, C. Ruckert, J. Steiner, R. Stevens, I. Thiele, O. Vassieva, Y. Ye, O. Zagnitko, and V.  
924 Vonstein. 2005. 'The subsystems approach to genome annotation and its use in the project to  
925 annotate 1000 genomes', *Nucleic Acids Research*, 33: 5691-702.

926 Pogoreutz, C., M. A. Gore, G. Perna, C. Millar, R. Nestler, R. F. Ormond, C. R. Clarke, and C. R. Voolstra.  
927 2019. 'Similar bacterial communities on healthy and injured skin of black tip reef sharks', *Anim*  
928 *Microbiome*, 1: 9.

929 Sabirova, JS, M Ferrer, D Regenhardt, KN Timmis, and PN Golyshin. 2020. 'Proteomic Insights into  
930 Metabolic Adaptations in *Alcanivorax borkumensis* Induced by Alkane Utilization', *Journal of*  
931 *Bacteriology*, 188: 3763-73.

932 Schlame, M., S. Brody, and K. Y. Hostetler. 1993. 'Mitochondrial Cardiolipin in Diverse Eukaryotes -  
933 Comparison of Biosynthetic Reactions and Molecular Acyl Species', *European Journal of*  
934 *Biochemistry*, 212: 727-35.

935 Schmieder, R., and R. Edwards. 2011. 'Fast Identification and Removal of Sequence Contamination from  
936 Genomic and Metagenomic Datasets', *Plos One*, 6.

937 Shadwick, R.E. , A.P. Farrell, and C.J. Brauner. 2015. *Physiology of Elasmobranch Fishes: Internal*  
938 *Processes* (Academic Press).

939 Speers-Roesch, B, and JR Treberg. 2010. 'The unusual energy metabolism of elasmobranch fishes.',  
940 *Comparative Biochemistry and Physiology Part A: Molecular & Integrative Physiology*, 155: 417-  
941 34.

942 Sullivan, T., and F. Regan. 2011a. 'The characterization, replication and testing of dermal denticles of  
943 *Scyliorhinus canicula* for physical mechanisms of biofouling prevention', *Bioinspiration &*  
944 *Biomimetics*, 6.

945 ———. 2011b. 'The characterization, replication and testing of dermal denticles of *Scyliorhinus canicula*  
946 for physical mechanisms of biofouling prevention', *Bioinspiration & Biomimetics*, 6: 046001.

947 Tahon, G., L. Lebbe, M. De Troch, K. Sabbe, and A. Willems. 2020. 'Leeuwenhoekiella aestuarii sp. nov.,  
948 isolated from salt-water sediment and first insights in the genomes of Leeuwenhoekiella  
949 species', *Int J Syst Evol Microbiol*, 70: 1706-19.

950 Tsutsui, S., Y. Dotsuta, A. Ono, M. Suzuki, H. Tateno, J. Hirabayashi, and O. Nakamura. 2014. 'A C-type  
951 lectin isolated from the skin of Japanese bullhead shark (*Heterodontus japonicus*) binds a  
952 remarkably broad range of sugars and induces blood coagulation.', *Journal of Biochemistry*, 157:  
953 345–56.

954 Vendl, C., T. Nelson, B. Ferrari, T. Thomas, and T. Rogers. 2021. 'Highly abundant core taxa in the blow  
955 within and across captive bottlenose dolphins provide evidence for a temporally stable airway  
956 microbiota', *BMC Microbiol*, 21: 20.

957 Verma, H., G. G. Dhingra, M. Sharma, V. Gupta, R. K. Negi, Y. Singh, and R. Lal. 2020. 'Comparative  
958 genomics of *Sphingopyxis* spp. unravelled functional attributes', *Genomics*, 112: 1956-69.

959 Wen, L., P. J. M. Thornycroft, J. C. Weaver, and G. V. Lauder. 2015. 'Hydrodynamic function of  
960 biomimetic shark skin: effect of denticle pattern and spacing', *Integrative and Comparative*  
961 *Biology*, 55: E196-E96.

962 Williams, T. J., H. Ertan, L. Ting, and R. Cavicchioli. 2009. 'Carbon and nitrogen substrate utilization in the  
963 marine bacterium *Sphingopyxis alaskensis* strain RB2256', *Isme Journal*, 3: 1036-52.

964 Wilson, B., B. S. Danilowicz, and W. G. Meijer. 2008. 'The diversity of bacterial communities associated  
965 with Atlantic Cod *Gadus morhua*', *Microbial Ecology*, 55: 425-34.

966 Yang, L., X. H. Wang, S. Cui, Y. X. Ren, J. Yu, N. Chen, Q. Xiao, L. K. Guo, and R. H. Wang. 2019.  
967 'Simultaneous removal of nitrogen and phosphorous by heterotrophic nitrification-aerobic  
968 denitrification of a metal resistant bacterium *Pseudomonas putida* strain NP5', *Bioresour*  
969 *Technol*, 285: 121360.

970 Zhang, D. Y., Y. Y. Li, X. Han, X. A. Li, and H. W. Chen. 2011. 'High-precision bio-replication of synthetic  
971 drag reduction shark skin', *Chinese Science Bulletin*, 56: 938-44.

972 Zheng, Q., W. X. Lin, Y. T. Liu, C. Chen, and N. Z. Jiao. 2016. 'A Comparison of 14 *Erythrobacter* Genomes  
973 Provides Insights into the Genomic Divergence and Scattered Distribution of Phototrophs',  
974 *Frontiers in Microbiology*, 7.

975